2010

Ion-sensitive field effect transistor (ISFET) for MEMS multisensory chips at RIT

Murat Baylav

Ion-Sensitive Field Effect Transistor (ISFET) for MEMS Multisensory Chips at RIT

By

Murat Baylav

A Thesis Submitted

In Partial Fulfillment

of the Requirements of the Degree of
Master of Science
in Microelectronic Engineering

Approved by:

Professor _____ Date: _____
Dr. Lynn F. Fuller (Thesis Advisor)

Professor _____ Date: _____
Dr. Karl D. Hirschman (Thesis Committee Member)

Professor _____ Date: _____
Dr. Santosh K. Kurinec (Thesis Committee Member)

Professor _____ Date: _____
Dr. Robert Pearson (Director, Microelectronic Engineering Program)

Professor _____ Date: _____
Dr. Sohail Dianat (Chair, Electrical and Microelectronic Engineering Department)

DEPARTMENT OF ELECTRICAL & MICROELECTRONIC ENGINEERING
KATE GLEASON COLLEGE OF ENGINEERING
ROCHESTER INSTITUTE OF TECHNOLOGY
ROCHESTER, NEW YORK
OCTOBER 2010

Acknowledgment

Throughout my education at RIT, I have been blessed with many amazing instructors and caring friends. I would have liked to thank each and every one of them. I would like to thank Dr. Santosh Kurinec for believing in me, giving me the opportunity of being a part of RIT, and also for passing her enthusiasm and knowledge in semiconductor field. I will be thankful to you for the rest of my life. I would like to thank Dr. Lynn Fuller for giving me the privilege of working for him in this exciting project. I would like to thank Ivan Puchades for being such a good friend and sharing his knowledge and time with me anytime I was in need. I want to thank my dear friends Heidi Purrington, Ellen Sedlack, Archana Devasia, Germain Fenger, Team Galt members Tal Nagourney and Jake Leveto for their friendship and amazing contributions to my project. I would like to thank my valued instructors Dr. Karl Hirschman and Dr. Robert Pearson for being in my committee and also contributing to my education. I would like to thank Sara Widlund for helping us in every step we take at RIT and also for sincerely caring about us. I would also like to thank all my instructors who helped me to get to where I am today. I would love to thank my Mom and my brother Burak Baylav for being my rocks and supporting me in each and every step I take in my life. Words would not suffice to express my love and gratitude for you. Finally, I would like to thank God for giving me the will to keep on and the blessings for which I am thankful every single day of my life.

Abstract

This study involves the design and fabrication of an Ion-Sensitive Field Effect Transistor (ISFET), which is aimed to be incorporated into the multisensory chips fabricated at RIT. ISFETs are used for various purposes in biomedical, medicine, and chemical applications and have advantages such as small size, low power consumption, robustness, and fast response time, over the ion-selective electrode (ISE) counterparts. The capability of fabricating ISFETs in a standard CMOS process let them to be used in sensor systems together with the dedicated signal processing circuitry which in turn makes portable applications possible. The ISFET fabricated in this study have a SiO_2 gate oxide and on top of that a Si_3N_4 layer. The latter layer, in addition to passivating the device, serves as a pH sensitive membrane. The overall process has 5 mask levels and the electrical tests, which were performed using buffer solutions with varying pH values, indicated that the transistor can be employed to measure the pH of solutions. ISFETs were also tested against environmental conditions such as temperature, long term exposure to various pH-valued solutions and it is found out that the FETs are quite robust in terms of temperature stability and long term drift. In addition to their pH sensing properties, these devices were also taken one step ahead to sense chloride ion (Cl^-) concentration via preparing a Cl^--sensitive membrane stacked on top of the Si_3N_4 layer. Electrical tests, which were performed in solutions with various Cl^- concentrations, showed that the modified ISFETs are also Cl^- sensitive.

Table of Contents

List of Figures

List of Tables

Chapter 1

Introduction

Measurement of pH (power of hydrogen) of solutions holds great importance for environmental and biomedical applications since a change in pH is one effective way to track chemical processes, which take place in nature. A common method to measure pH is the well-known glass membrane electrode which is shown in Figure 1.1; however, glass membrane electrode comes with some limitations such as the inability to operate at high temperatures, being a bulky device (which prevents its use in vivo monitoring), manufacturing difficulties, and low durability. However, development of Ion Sensitive Field Effect Transistor (ISFET) concept by P. Bergveld in 1970 [1, 2] introduced a remedy for these short comings. Since the introduction of ISFETs, hundreds of studies have been reported in literature exploiting various uses of the device. In addition to the pH sensing properties of the gate insulator of ISFETs, researchers also have shown the capability of the ISFET to sense other ions via using ion-specific membranes atop of the gate insulator [3].

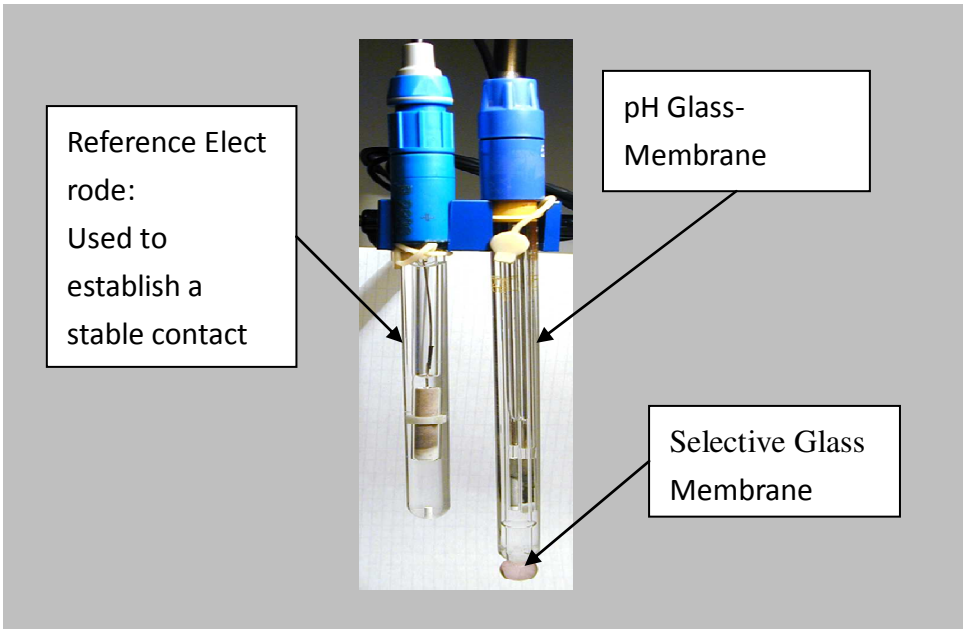

Figure 1.1: Glass membrane electrode paired with a reference electrode.

ISFETs are realized by removing the metal gate electrode of a Metal Oxide Field Effect Transistor (MOSFET). Therefore, the metal becomes a remote gate. The gate insulator, which is commonly silicon dioxide (SiO_2), is exposed to an ionic solution (electrolyte), which modulates the threshold voltage, $V_{T,}$ of the transistor [1-3]. Figure 1.2 is illustrating this modification to the MOSFET and the resulting ISFET structure. The modulation in device threshold voltage is explained as a result of the interaction of the insulating material with the ions in the electrolyte. The interaction reveals itself as a change in the conductivity of the underlying channel and hence in the current flowing through it.

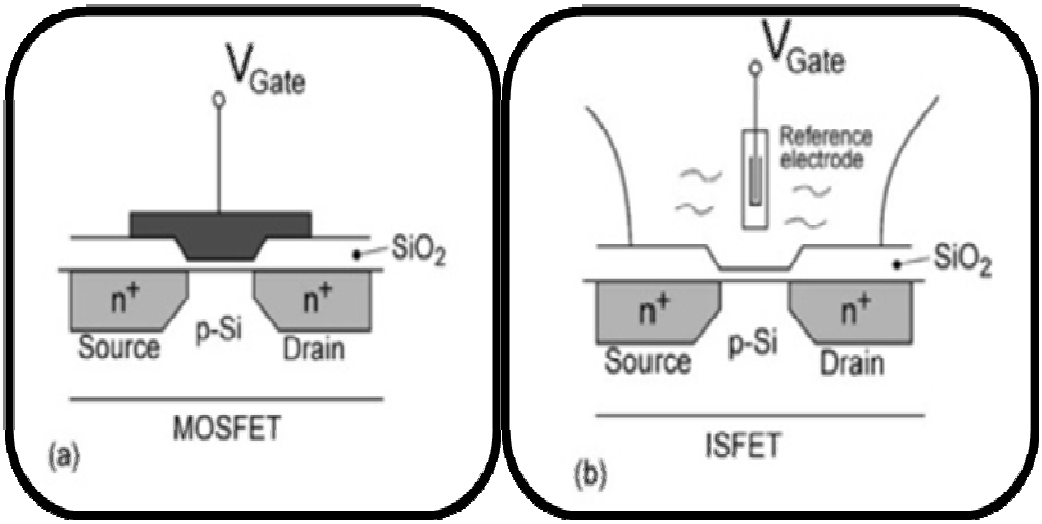

Figure 1.2: Modifications to MOSFET. (a) A typical MOSFET structure. (b) Resulting ISFET device [3].

Aside from having a slightly different structure than a regular MOSFET; same equations could be applied to the ISFET with one exception. The threshold voltage equation had to be modified to include the effect of pH of the electrolyte [3]. Therefore, various studies followed this invention to understand the chemistry in the electrolyte-insulator interface and to develop useful models that accurately characterize the change in the threshold voltage of the ISFET.

This thesis reviews the fundamentals of ISFET concept by starting from the electrochemistry of electrolytes, the pH concept, pH sensing insulators employed on ISFETs, and their comparison. These are explained in this chapter. In chapter 2, electrolyte-insulator-semiconductor (EIS) structure is explained in detail with the chemical treatment of electrolyte-insulator interface by using the site-dissociation theory and the double layer theory of Gouy-Chapman-Stern [4, 5]. Also in chapter 2, the results

of the EIS analyses are used to derive a pH sensitivity expression for the ISFET. In addition, a method of changing the sensitivity of an ISFET to other ions by using dedicated membranes is also explained. Chapter 3 presents the theory of ISFET with fundamental equations which characterize its operation. Moreover, the ISFET structure employed in this study and the dedicated mask design with the process flow are also a part of Chapter 3. Chapter 4 talks about the electrical and environmental tests performed on the test structures and, finally, Chapter 5 presents conclusions on the results and their impact on RIT's success in fabricating ISFETs.

1.1. Electrochemistry of Ionic Solutions (Electrolytes)

Investigation of ion activity (concentration) or chemical compounds are performed in electrolytes (ionic solutions). These solutions are prepared by dissolving chemical compounds in polar solvents such as water. Water is one of the most common solvent since its molecules are not symmetrically charged. Therefore, water has a certain dipole moment. This dipole moment weakens the chemical bonds of the compounds and has them dissolve. Dissolved ions are surrounded by as enough water molecules as to screen their charge. This mechanism changes the dielectric constant around the ions and

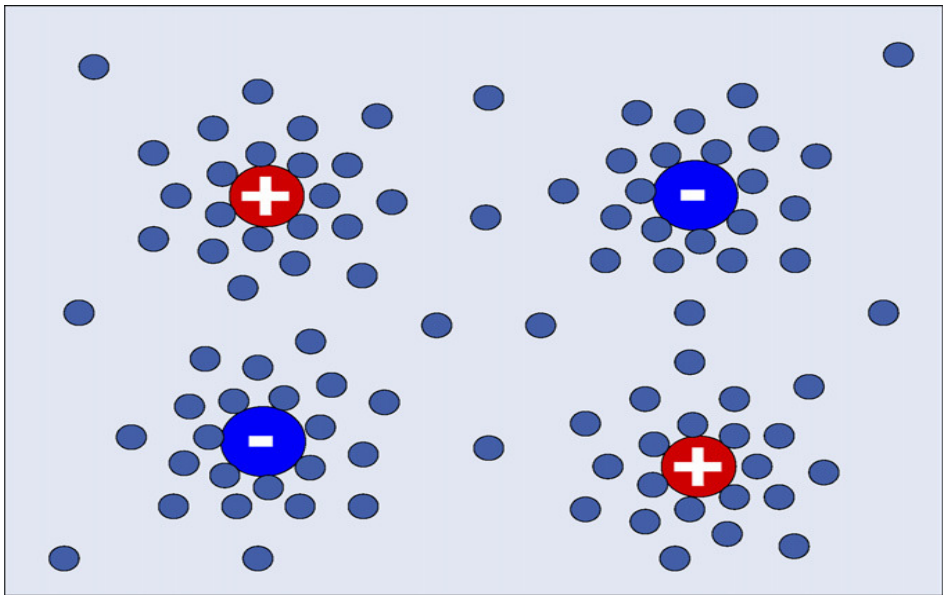

Figure 1.3: Dissolved free ions surrounded by water molecules [6].

prevent them from being influenced by the electric fields in the surrounding. Therefore, the ions become free to move in the solution and conduct electric current [6]. Figure 1.3 shows this mechanism for an electrolyte in which free ions of a dissolved salt exist.

1.2. Concept of pH (Power of Hydrogen)

In electrolytes, not only the compounds but the water molecules dissolve to some extent, as well. This mechanism is governed by the following equation which reaches to equilibrium in time:

$$H_2O \Longleftrightarrow H^+ + OH^- \qquad (1.1)$$

Equilibrium constant in terms of molar concentrations, moles per liter, of the species for the chemical equation (1.1) is given as [6]:

$$K_{eq} = \frac{\left[\mathrm{H^+}\right]\left[\mathrm{OH^-}\right]}{\left[\mathrm{H_2O}\right]} \tag{1.2}$$

Assuming the density of water constant, individual concentrations of hydrogen and hydroxyl ions can be calculated as given in equation (1.3), and by moving from this, dissociation constant, K_w, can be found as given in equation (1.4).

$$K_{eq} = \frac{\left[\mathrm{H^+}\right]\left[\mathrm{OH^-}\right]}{1\ \mathrm{g/mL} \times 1\ \mathrm{mol}/18\ \mathrm{g}} = \frac{\left[\mathrm{H^+}\right]\left[\mathrm{OH^-}\right]}{55.56\ \mathrm{M}} \tag{1.3}$$

$$K_w = K_{eq} \times 55.56 = \left[\mathrm{H^+}\right]\left[\mathrm{OH^-}\right] \tag{1.4}$$

K_w has a constant value of 10^{-14} at room temperature. However, in chemistry it is more convenient to work with these ion concentrations in terms of logarithmic values. Taking the logarithm of equation (1.4) results in the sum of powers of individual ions is equal to 14 as shown in equation (1.5).

$$\log_{10}\left(\left[H^{+}\right]\left[OH^{-}\right]\right) = pH+pOH=14 \quad (1.5)$$

In chemistry, solutions with a pH of 7 are defined as neutral. As the amount of hydrogen ions increase, acidity increases and solution becomes low in pH. On the other hand, as the amount of hydroxyl ions increase, concentration of hydrogen ions decreases due to the relationship given in equation (1.5). Therefore, solution becomes basic and has a pH value higher than 7. Solutions with very low pH values are named as strong acids while the solutions with very high pH values are named as strong bases. Understanding the concept of pH is crucial, since the concentration of these ions is what is affecting the operation of ISFET.

1.3. pH Sensing Insulators

In pH measurements, pH sensitive insulator plays the most important role. It is this layer that actually interacts with the electrolyte. A good pH sensitive insulator must possess linear response in a wide pH range, must show high selectivity to hydrogen ions and less selectivity other ions. It must have high sensitivity to concentration changes of hydrogen ions and also must exhibit low drift performance. First pH sensitive insulator, which was used on the ISFET, was the SiO_2. Actually, SiO_2 was the already existing gate

dielectric of a regular MOSFET [1, 2]. Therefore, this resulted in comparisons with the glass membrane electrode, which was requiring its porous glass membrane be hydrated to allow hydrogen ion transfer to either sides of the membrane [3]. However, Matsuo [7] already used Si_3N_4 (stacked atop SiO_2), which was an insulator that did not hydrate. This experiment showed that the pH sensitivity of the gate insulator was a result of pure surface phenomena occurring in the electrolyte-insulator interface. Therefore, researchers focused on this interface to explain this phenomenon and model it. Yates et al. [4] worked on the colloidal oxide-water interfaces and explained double layers formed in these interfaces with site-binding theory, which will be explained further in next chapter. Afterwards, Bousse et al. [5] applied those models to electrolyte/insulator/silicon (EIS) interfaces and developed a very accurate model with two parameters, namely pH_{pzc} and β, which were the pH value of the electrolyte at which the insulator surface was neutral and surface buffer capacity of the insulator, respectively. The latter parameter was also explaining the reason for the low pH sensitivity when compared to Nernstian sensitivity of the glass membrane electrode which was 58.2 mV/pH at 20 °C. The buffer capacity of the insulator is different for each insulator and resulting in different sensitivities to pH [3]. Matsuo also tested different insulators such as Al_2O_3, Ta_2O_5 and concluded that these

two insulators were showing the best sensitivity which was close to the ideal Nernstian sensitivity. Table 1.1 is illustrating the measured sensitivities by Yuqing [8].

Table 1.1 Measured pH sensitivities of insulators [8].

Insulators	Si_3N_4	Al_2O_3	Ta_2O_5
Measurement pH-Range	2-12	2-12	2-12
Measured Sensitivity (mV/pH)	53-55	54-56	56-58

Chapter 2

Electrolyte-Insulator-Semiconductor (EIS) Structure

Figure 2.1 illustrates the potential and charge distribution at the electrolyte-insulator interface of an ISFET. Inorganic oxides such as SiO_2, Si_3N_4, Al_2O_3, and Ta_2O_5 have amphoteric surface sites. These surface sites are the hydroxyl groups and they donate or accept H^+ ions from the solution acting as an acid or a base, depending on the bulk solution pH [9]. As a result of this interaction with the electrolyte, the surface of the insulator now has a net charge of σ_0 as shown in Figure 2.1. Moreover, the pH in the vicinity of the insulator surface differs from the pH in the bulk of the solution. The surface hydrogen ion concentration, $[H_s^+]$ is related to the bulk hydrogen ion concentration $[H_B^+]$ through a Boltzmann relationship given by:

$$\left[H_S^+\right] = \left[H_B^+\right] \exp\left(\frac{-q\psi_0}{kT}\right) \tag{2.1}$$

Taking the minus logarithm of both sides of equation (2.1) allow us to represent the relation in terms of pH and given as:

$$pH_S = pH_B + \frac{q\psi_0}{2.3kT} \tag{2.2}$$

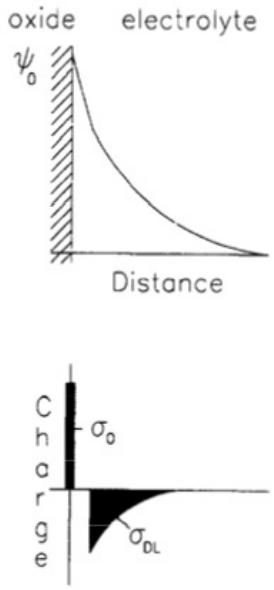

Figure 2.1: Potential profile and charge distribution for insulator-electrolyte interface [10].

Due to charge neutrality, the net charge σ_0 has to be compensated by the ions in the solution in the vicinity of the insulator surface. Typically, the ions in the solution have large radiuses and have a random thermal motion. Therefore, compensation of the surface charge can only be achieved by forming a diffuse layer of these charges extending to some distance from the insulator surface into the bulk of the solution [5].

2.1. Gouy-Chapman-Stern Model for Insulator – Electrolyte Interface

The potential drop ψ_0, shown in Figure 2.1 and given in equations (2.1) and (2.2) drops across this diffuse layer also known as the Gouy-Chapman double layer [6, 11, 12]. An example illustration of this diffuse layer of ions is shown in Figure 2.2.

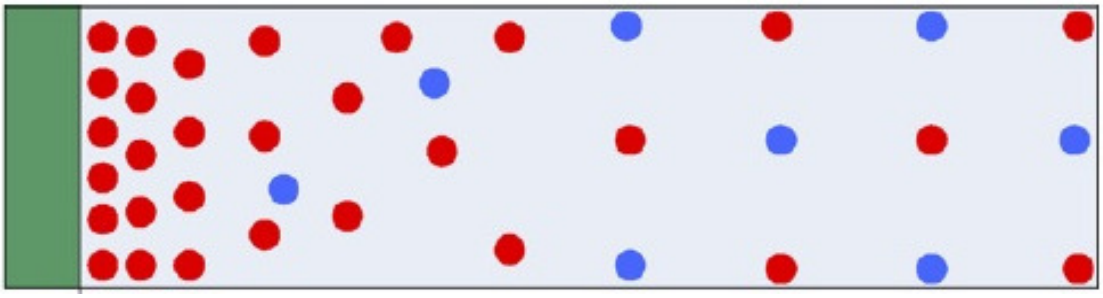

Figure 2.2: Gouy-Chapman double layer [6].

From Figure 2.1, it can be seen that the net surface charge σ_0 is compensated by the double layer charge σ_{DL} and the potential ψ_0 is actually the dropping over a diffuse layer capacitance, C_{df} [9]. However, experimentally it was shown that Gouy-Chapman diffuse layer model, which was applied to insulator-electrolyte interface, was over-estimating the diffuse layer capacitance and the interface charge [6, 11]. The reason for that was the treatment of ions in the solution as point charges which can approach the insulator surface to a distance lower than their large atomic radius. As explained in the first chapter, these ions are free to move in the solution with the help of the agglomeration of water molecules around them. This over-estimation in the treatment of insulator-electrolyte interface was mitigated by Stern [12]. Figure 2.3 presents a useful interpretation of the improved model, Gouy-Chapman-Stern model, for a metal-electrolyte structure which is valid also for insulator-electrolyte as will be seen later in this chapter.

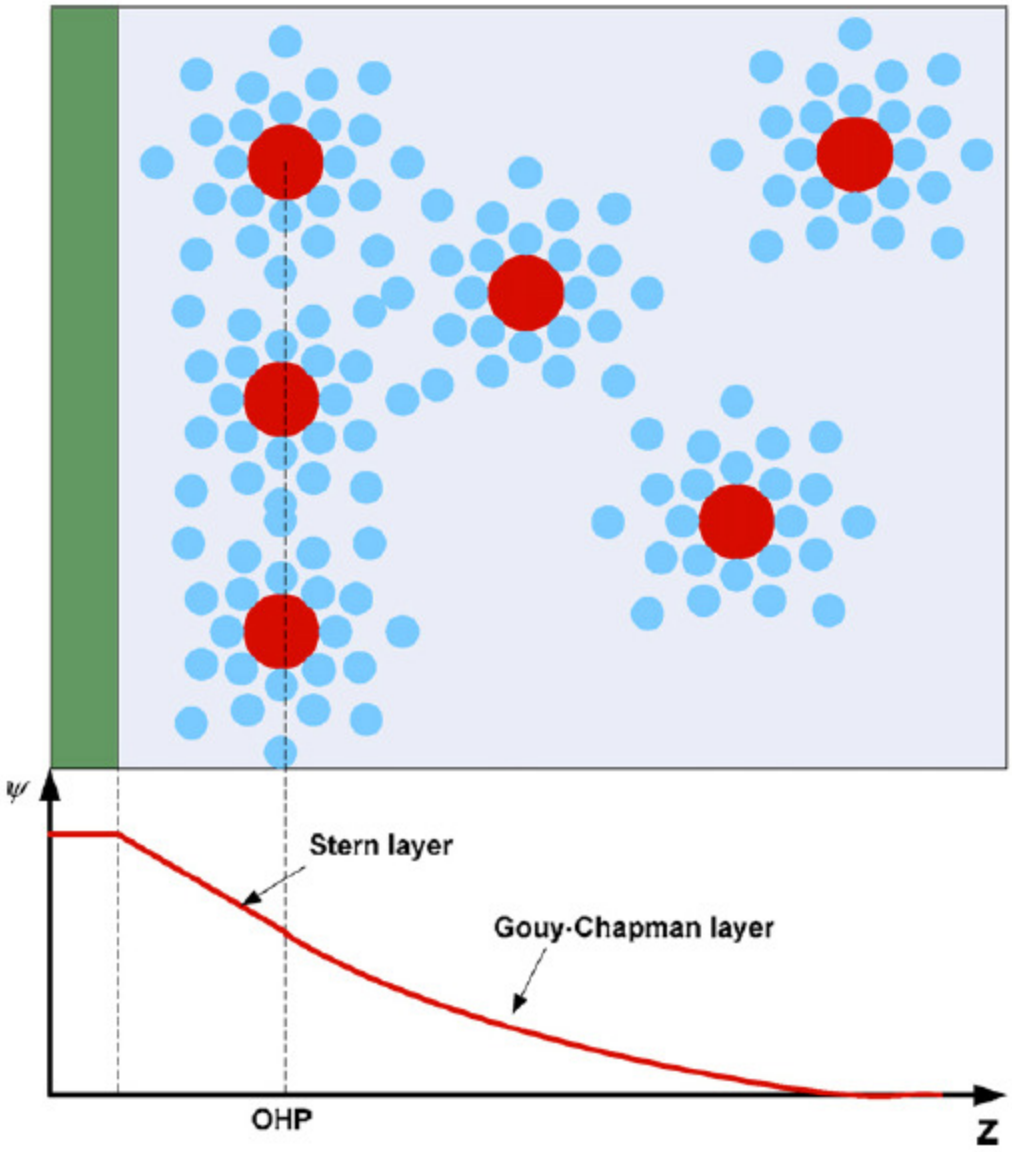

Figure 2.3: Representation of Gouy-Chapman-Stern model [6].

Here, the closest approach of an ion can be only its radial distance had it been not surrounded by water molecules. The first layer of ions is placed in the so called outer Helmholtz plane (OHP). The potential drops starting from the surface and becomes zero deep in the bulk solution. Between the insulator surface and the OHP there is no ionic charge and this results in a constant capacitance called Stern capacitance, C_{st}, which is in

series with the Gouy-Chapman double layer capacitance, C_{df}. It has a constant value of 20 $\mu F/cm^2$ [13] and becomes the dominant capacitance with respect to C_{df} which is an order of magnitude greater than that. However, in the overall electrolyte-insulator-semiconductor (EIS) structure, the series of these capacitance together with the insulator capacitance C_{ox} results in a lower equivalent capacitor due to the respectively very low capacitance of the insulator layer.

Gouy-Chapman double layer capacitance and the Stern capacitance are two out of the three components of the potential drop, ψ_0, of the insulator-electrolyte interface. The last component is the net charge built on the surface of the insulator, σ_0, as a result of the surface chemistry. Site-dissociation model has been used since 1970s to explain the charging mechanism of insulator surface and use in expressions for ISFET operation as will be seen in next Chapter 3.

2.2. Site-Dissociation Model for Insulator Surface Charging

According to this model, chemical reactions between the insulator surface and the electrolyte can only happen inside the OHP and the ions of the dissolved species (salts) of the electrolyte cannot approach to the insulator surface as explained in the previous section. The only species that can approach to the surface of the insulator is the hydrogen

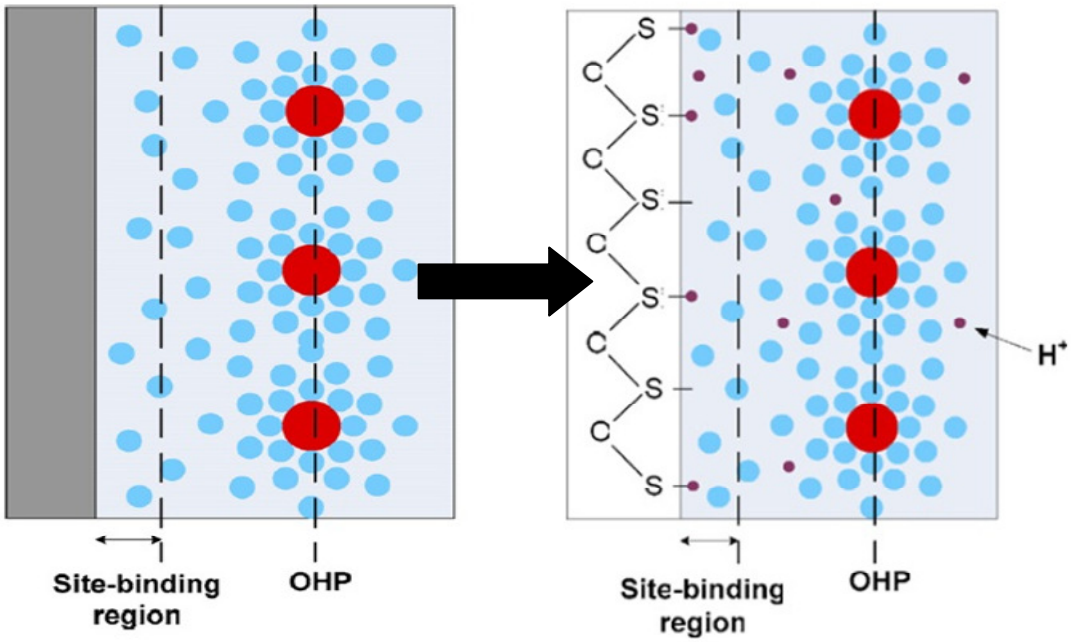

Figure 2.4: Site-dissociation and binding model representation [6].

ions, H^+, since these ions are small and not surrounded by water molecules or not hydrated by water molecules. Figure 2.4 illustrates this reasoning for the capability of only hydrogen ions to come contact with the insulator surface. The picture is given for SiO_2 surfaces but is also valid for other inorganic oxides since they all have these surface amphoteric sites accepting and/or donating hydrogen ions from and to the electrolyte.

Acid-base behavior of the surface of the insulator determines how sensitive the ISFET to changes in the pH of the bulk electrolyte. Chemical reactions which result in charging of the surface and different pH value in the vicinity of the insulator surface are given as:

$$\text{A-OH} \overset{K_a}{\Longleftrightarrow} \text{A-O}^- + \text{H}_S^+ \tag{2.3}$$

$$\text{A-OH} + \text{H}_S^+ \overset{K_b}{\Longleftrightarrow} \text{A-OH}_2^+ \tag{2.4}$$

Dissociation constants which are intrinsic to an insulator are given as:

$$\text{K}_a = \frac{\left[\text{A-O}^-\right]\left[\text{H}_S^+\right]}{\left[\text{A-OH}\right]} \tag{2.5}$$

$$\text{K}_b = \frac{\left[\text{A-OH}_2^+\right]}{\left[\text{A-OH}\right]\left[\text{H}_S^+\right]} \tag{2.6}$$

K_a and K_b define the acid-base behavior of the insulator surface [9]. [A-OH], [$A\text{-}OH_2^+$], and [$A\text{-}O^-$] are the number of neutral, positive and negative surface sites per cm^2, respectively. These sites are randomly distributed over the surface of the insulator and their numbers are solely determined by the equilibrium constants and the pH of the bulk electrolyte which is given as pH_B in equation (2.2). The number of the hydrogen concentration in the vicinity of the insulator interface is given by [H_S^+] and also given in terms of its power in equation (2.2) as pH_S. As mentioned earlier, [H_S^+] is related to [H_B^+] through Boltzmann relationship with the potential drop ψ_0 across the interface as a result of the net charge formed on the surface through equations (2.3) and (2.4).

From equations (2.5) and (2.6), $[H_S^+]$ can be derived as:

$$\left[H_S^+\right]^2 = \frac{K_a}{K_b}\frac{\left[A\text{-}OH_2^+\right]}{\left[A\text{-}O^-\right]} \tag{2.7}$$

In addition to being an expression for $[H_S^+]$, equation (2.7) also gives information on another important parameter, namely, pH_{pzc} which is also intrinsic to each type of insulator. This parameter is defined as the pH at point of zero charge which is the pH value of the bulk solution at which the surface of the insulator is neutral. The reasoning is that, if the surface of the insulator is neutral, then, then $[A\text{-}OH_2^+]$ must be equal to $[A\text{-}O^-]$. In this case, σ_0 is zero therefore, so is ψ_0. From equation (2.7)

$$\left[H_S^+\right] = \sqrt{\frac{K_a}{K_b}} \tag{2.8}$$

and from equation (2.1)

$$\left[H_S^+\right] = \left[H_B^+\right] = \sqrt{\frac{K_a}{K_b}} \tag{2.9}$$

and finally, pH_{pzc} is given as:

$$pH_{pzc} = -\log\left(\left[H_S^+\right] = \left[H_B^+\right]\right) = -\log\left(\sqrt{\frac{K_a}{K_b}}\right) \tag{2.10}$$

When the pH of the bulk solution differs than pH_{pzc}, the response of the insulator surface to this change is an indicator of how pH sensitive it is. The sensitivity is expressed in terms of the buffer capacity of the surface and indicated with the symbol β. Buffer capacity is defined as the ability of the insulator surface to buffer the minuscule changes in the surface pH_s. It is given as the ratio of the change in the number of the charged surface groups to the change in the pH_s [9, 10]. Therefore, expressed as:

$$\beta = \frac{d[\mathrm{B}]}{d\mathrm{pH_S}} \tag{2.11}$$

where, [B] represents the amount of net charge on the insulator surface and can be given as:

$$[\mathrm{B}] = \left[\mathrm{A\text{-}O^-}\right] - \left[\mathrm{A\text{-}OH_2^+}\right] = -\frac{\sigma_0}{q} \tag{2.12}$$

Total surface sites, N_S, can be given as the sum of the charged and the neutral sites as:

$$\mathrm{N_S} = \left[\mathrm{A\text{-}O^-}\right] + \left[\mathrm{A\text{-}OH_2^+}\right] + \left[\mathrm{A\text{-}OH}\right] \tag{2.13}$$

Using equations (2.5), (2.6), and (2.13) the charged sites can be expressed by the following equations as:

$$\left[\mathrm{A\text{-}O^-}\right] = \mathrm{N_S}\frac{\mathrm{K_a}}{\mathrm{K_a} + \left[\mathrm{H_S^+}\right] + \mathrm{K_b}\left[\mathrm{H_S^+}\right]^2} \tag{2.14}$$

$$\left[\mathrm{A\text{-}OH_2^+}\right] = \mathrm{N_S}\frac{\mathrm{K_b}\left[\mathrm{H_S^+}\right]^2}{\mathrm{K_a} + \left[\mathrm{H_S^+}\right] + \mathrm{K_b}\left[\mathrm{H_S^+}\right]^2} \tag{2.15}$$

From equations (2.10), (2.11), (2.12), (2.14), and (2.15) the buffer capacity of the insulator surface can now be expressed as:

$$\begin{aligned}\beta &= \frac{d\left[\mathrm{B}\right]}{d\mathrm{pH_S}} = \frac{d\left[\mathrm{B}\right]}{d\left[\mathrm{H_S^+}\right]} \cdot \frac{d\left[\mathrm{H_S^+}\right]}{d\mathrm{pH_S}} \\ &= 2.3 \cdot \left[\mathrm{H_S^+}\right] \cdot \mathrm{N_S} \cdot \frac{\mathrm{K_a} + 4\mathrm{K_a}\mathrm{K_b}\left[\mathrm{H_S^+}\right] + \mathrm{K_b}\left[\mathrm{H_S^+}\right]^2}{\left(\mathrm{K_a} + \left[\mathrm{H_S^+}\right] + \mathrm{K_b}\left[\mathrm{H_S^+}\right]^2\right)^2}\end{aligned} \tag{2.16}$$

Taking the logarithm of (2.1) results in an expression for ψ_0 in terms of pH_S and pH_B. and given as:

$$\psi_0 = 2.3\frac{kT}{q}\left(pH_S - pH_B\right) \tag{2.17}$$

ψ_0 charges the equivalent capacitance, C_e, which is the series combination of C_{df} and C_{st}. Therefore, the surface charge, σ_0 can be expressed as:

$$\sigma_0 = -\psi_0 C_e = -\sigma_{DL} \tag{2.18}$$

Equation (2.17) will be the key equation to formulating the final expression relating the ψ_0 to changes in the bulk pH, which is pH_B. However, the sensitivity of this potential to changes in pH_B is actually coming from the induced changes in pH_S which is actually determined by the buffer capacity of the insulator and the equivalent capacitance over which this potential drops. Using equations (2.11), (2.12), and (2.18) the sensitivity of ψ_0 to pH_S can be written as:

$$\frac{d\psi_0}{dpH_S} = \frac{d\sigma_0}{dpH_S}\cdot\frac{d\psi_0}{d\sigma_0} = \frac{-q\beta}{C_e} \tag{2.19}$$

Examining equation (2.16) and (2.19) results in important conclusions as to how the type of insulator used in an ISFET affects the final sensitivity of ψ_0 to changes in pH_S and finally in pH_B. Provided that C_{eq} is small a large sensitivity can be achieved with a high buffer capacity, β. A high β can be achieved with a large amount of surface sites, N_S, and dissociation constants, K_a and K_b. In the following section, the final form of the sensitivity expression for insulator surface and, therefore, ISFET device is derived. The final sensitivity equation relates the changes in ψ_0 to pH of the bulk solution and incorporates the effect of the chosen insulator type due to the parameters examined in this section. These effects are lumped into a sensitivity factor represented by α, which also explains the sub-Nernstian sensitivity of some insulators compared to glass membrane electrodes [3].

2.3. pH Sensitivity of ISFETs

Since ISFET concept was proposed, for the first time by Bergveld in 1970s, all attempts have been made to model the sensitivity of the potential drop ψ_0 to the changes pH of the bulk solution. After all, assuming everything else is constant, any change in this potential drop has to be compensated by the semiconductor surface potential ψ_s, therefore, the threshold voltage of the FET. The reason is that during normal operation

ISFET is biased by a fixed gate potential. Thus, as will be seen in Chapter 3, an expression for sensitivity of ψ_0 to pH has to be incorporated to the equations defining the ISFET operation. In order to do so, equation (2.17) can be used. Taking the derivative of ψ_0 with respect to pH_B results in

$$\frac{d\psi_0}{d\mathrm{pH_B}} = 2.3\frac{kT}{q}\left(\frac{d\mathrm{pH_S}}{d\mathrm{pH_B}} - 1\right) \tag{2.20}$$

and, expanding the derivative of pH_S with respect to pH_B to make use of the relationships of the previous section gives

$$\frac{d\psi_0}{d\mathrm{pH_B}} = 2.3\frac{kT}{q}\left(\frac{d\mathrm{pH_S}}{d\psi_0}\frac{d\psi_0}{d\mathrm{pH_B}} - 1\right) \tag{2.21}$$

Rearranging (2.21) and using equation (2.19) results in the pH sensitivity equation of an ISFET device given as:

$$\frac{d\psi_0}{d\mathrm{pH_B}} = -2.3\frac{kT}{q}\frac{1}{2.3\frac{kT}{q^2}\frac{C_e}{\beta}+1} = -2.3\alpha\frac{kT}{q} \tag{2.22}$$

The term α is the sensitivity parameter of the ISFET gate insulator to pH of the bulk solution. It can have a maximum value of 1 depending on the insulator type chosen [3]. This is due to the fact that, α, involves the terms intrinsic buffer capacity and equivalent capacitance of the insulator-electrolyte interface. As mentioned earlier, buffer capacity is a function of the number of the surface sites ready to interact with the hydrogen ions in the vicinity of the surface, and it is also a function of the dissociation constants K_a and K_b. If the maximum sensitivity, the Nernstian sensitivity of 59.3 mV/pH at 25 °C, is needed, then, the insulator needs a very high buffer capacity so that α goes to 1. In addition to that, the value of C_e should be low irrespective of the ion concentration of the electrolyte since as the ion concentration increases the value of this capacitance tends to increase and reduce the sensitivity of the threshold voltage of the ISFET to pH.

Measuring β and C_e individually is not an easy thing to do, however the sensitivity α can be extracted from the response plot of ISFET to pH. The sensitivity of these oxides and also the effect of ion concentration was investigated by Bergveld and his

group and it was found to be SiO_2 was showing the lowest pH sensitivity and the sensitivity was affected adversely as the ion concentration of the electrolyte was increased. On the other hand, Ta_2O_5 had a very high buffer capacity such that, even when the ion concentration of the electrolyte was increased, the pH sensitivity of the ISFET was not changing much. Figure 2.5 shows the experimental plots generated as a result of these experiments on different insulator types.

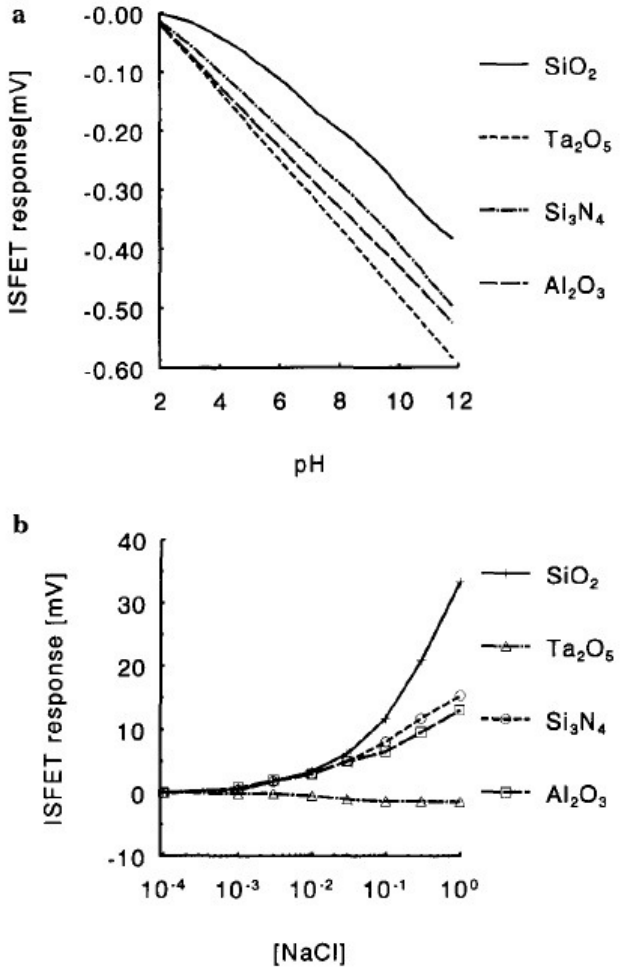

Figure 2.5: (a) ISFET response to electrolyte pH at constant ion concentration. (b) ISFET response to ion concentration at constant pH [3].

2.4. Making ISFETs Sensitive to Different Ions

So far, it has been discussed that the sensitivity of the insulator surfaces to the hydrogen ion concentration is what makes an ISFET useful for pH detection. However, the applications of ISFET are not limited to only pH detection but, over the years, ISFETs are employed for detection of different ions, as well. How this is possible is the topic of this section. After all, this thesis study also involves the fabrication of a chloride ion, Cl^-, sensitive ISFET which can be employed in water quality sensory system here at RIT. As mentioned earlier, large ions cannot approach to the surface of the insulator where chemical reactions can occur with hydrogen ions and the insulator surface. However, by preparing a selective reaction medium which will, ideally, only allow a specific ion to approach closer to the insulator surface and change the local hydrogen ion concentration is the solution for achieving ISFETs sensitive to different ions [6]. Therefore, after the invention of ISFETs, many researchers developed membranes which are selective to an ion of interest and deposited them o top of the gate insulator. Figure 2.6 is an illustration of this idea where a membrane on top of the insulator allows the ion of interest to approach to the insulator. Within the membrane, the ions, naturally, react with the water molecules and change the local pH of the interface. This practice results for the insulator surface to, indirectly, be sensitive to the concentration of the ion

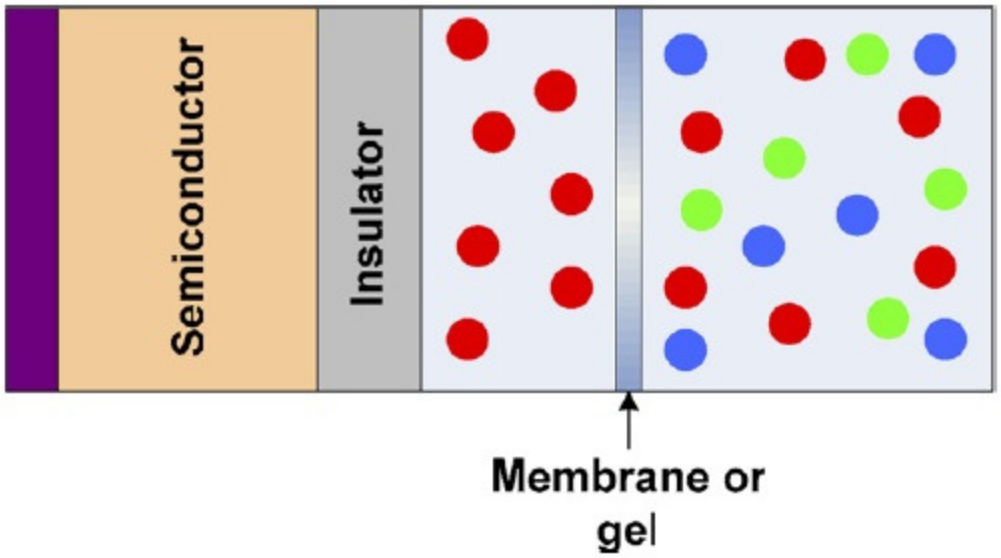

Figure 2.6: Application of membranes for ISFETs sensitive to different ions [6].

of interest. In this study, this is also the same approach which was followed. A membrane, which is selective to chloride ions, was prepared with the recipe developed by [14] and deposited on top of the Si_3N_4 surface.

Chapter 3

ISFET Operation and Technology

3.1. ISFET Operation as an Electronic Device

ISFET can be regarded as a MOSFET whose gate connection is replaced by the metal connection of a reference electrode, which is immersed in the electrolyte to be analyzed. The electrolyte includes the ions of interest and forms the conducting medium between the reference electrode and the membrane/gate-insulator stack. Figure 3.1 illustrates the difference between a MOSFET and ISFET schematically [3]. As can be seen from Figure 3.1(c), both MOSFET and ISFET devices have the same electrical representation, however, unlike the case of a MOSFET, ISFET cannot be totally encapsulated. The gate has to be left open so that it is in direct contact with the electrolyte to be analyzed. Due to the similarity in the structure of the ISFET and MOSFET explained and illustrated in Figure 3.1(c), the operation of an ISFET starts with analyzing the theoretical description of a MOSFET. During normal operation, ISFETs are biased in non-saturated mode, since any change in ion concentration in the solution is assumed to modulate the threshold voltage which, in this mode of operation, exhibits a linear relation with drain current.

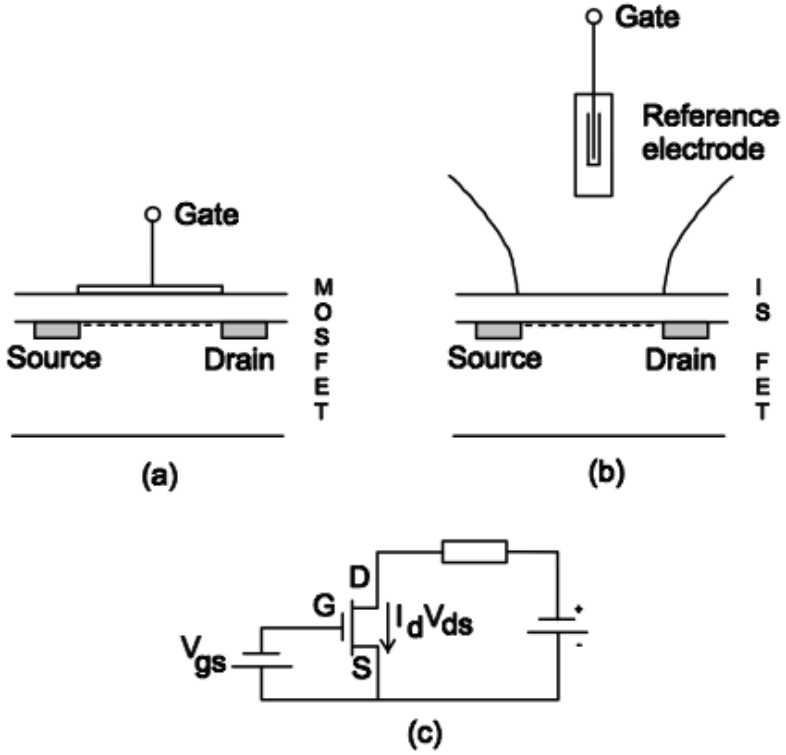

Figure 3.1: (a) Schematic diagram of a MOSFET. (b) Schematic diagram of an ISFET. (c) Electrical representation of both MOSFET and ISFET [3].

Drain current of a MOSFET, in non-saturated mode, can be expressed as:

$$I_{DS} = C_{ox}'\mu\frac{W}{L}\left[\left(V_{GS}-V_T\right)V_{DS}-\frac{1}{2}{V_{DS}}^2\right] \tag{3.1}$$

where, C_{ox}' is the oxide capacitance per unit area, W and L are the channel width and length, respectively, μ is the effective surface mobility, and V_{GS}, V_{DS}, and V_T are the gate-

to-source, drain-to-source, and threshold voltage, respectively. Threshold voltage of the MOSFET is expressed as:

$$V_T = \left(\frac{\Phi_M - \Phi_{Si}}{q} - \frac{Q_{ox}'}{C_{ox}'} \right) + 2\phi_{FB} - \frac{Q_B'}{C_{ox}'} \tag{3.2}$$

where, the term in the parenthesis is the flat band voltage V_{FB} which is composed of the metal-semiconductor work function difference Φ_M and Φ_{Si} and any oxide charge/surface state per unit area introduced during the process. Q_B' is the depletion charge per unit area and the φ_{FB} is the Fermi potential of the bulk silicon.

For an ISFET manufactured with the same process, two additional terms are incorporated into the threshold voltage of equation (3.2). These terms are the reference electrode potential E_{ref} and the interfacial potential at the electrolyte-insulator interface $\psi_0+\chi^{sol}$. In this study, an *Ag/AgCl* commercial reference electrode is used to bias the ISFETs. In addition, ISFETs are also biased with a gold (Au) wire in order to investigate the possibility of an integrated pseudo-reference electrode to be with for the ISFETs which are fabricated here at RIT. The *Ag/AgCl* electrode has a 0.205 V relative potential with respect to standard hydrogen electrode which forms the basis for all reference

electrodes. The standard hydrogen electrode has an absolute electrode potential of 4.7 V [15]. Thus, E_{ref} (*Ag/AgCl*) =4.905 V. ISFETs are investigated using aqueous solution, thus the solvent is water. In equation (3.3), ψ_0 is the potential drop across the electrolyte-insulator interface and, as mentioned in the previous chapter, is a strong function of pH of the bulk electrolyte and χ^{sol} is the surface dipole potential of the solvent. The reported values for χ^{sol} have a range between 0.1-0.2 V [16]. The expression for the threshold voltage of the ISFET then becomes:

$$V_T = \left(E_{ref} - \Psi(\mathrm{pH}) + \chi^{sol} - \frac{\Phi_{Si}}{q} - \frac{Q_{ox}'}{C_{ox}'} \right) + 2\phi_{FB} - \frac{Q_B'}{C_{ox}'} \tag{3.3}$$

Figure 3.2(a) illustrates a family of curves generated by biasing an ISFET, immersed in an aqueous solution of pH=2, through a reference electrode (also immersed in the electrolyte). Id vs. VDs curves for various V_{GS} values prove the operation of ISFET just like a MOSFET. In addition, in Figure 3.2(b), the same curves were generated with the reference electrode grounded (V_{GS}=0 V) and the pH of the solution was varied. This result can be attributed to a change in threshold voltage, and from (3.3) it can be observed that the change is due to the potential drop ψ_0 which is a function of pH.

Therefore, in ISFET applications, the main goal is to represent the relation between ψ_0 to the pH of the solution. However, ψ_0 is not only affected by the pHof the electrolyte but also, as explained in Chapter 2, the type of the membrane that is in contact with the electrolyte.

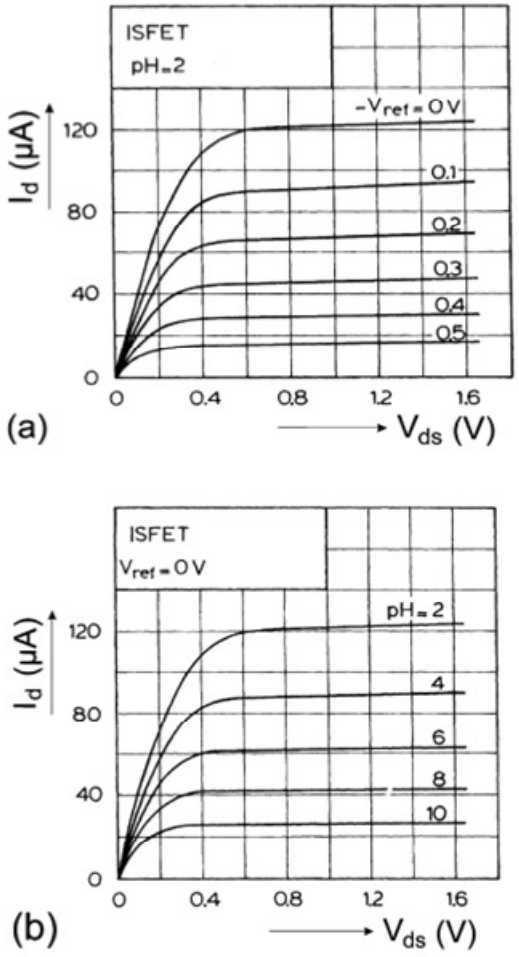

Figure 3.2: (a) Family of curves with VGS varied at pH=2. (b) Family of curves at VGS= 0V and pH varied [3].

As mentioned earlier, the first material used as a pH sensitive membrane was SiO_2 which was inherently a part of the MOSFET technology and doing so resulted in comparisons with other potentiometric ion sensors such as pH glass-membrane electrode.

In order for a pH glass-membrane electrode to become pH sensitive, the membrane requires to be hydrated. However, it was proved that implementing the membrane via using a Si_3N_4 membrane, which does not hydrate, was also possible [7]. In this case, not only the threshold voltage of the ISFET was sensitive to pH, but the sensitivity, $\Delta V_T / \Delta pH$, was closer to the maximum Nernstian sensitivity of 58.2 mV per decade at 20 °C (Nernstian sensitivity is the pH sensitivity of the conventional potentiometric ion sensors such as pH glass-membrane electrode and sets the maximum limit for the sensitivity for an ISFET. By applying different membranes, the sensitivity of an ISFET can be increased closer to this target). Original equation for Nernstian sensitivity is given in Appendix A in the context of pH glass-membrane electrode. From the nitride membrane results, it was concluded that one had to consider a pure surface phenomena at the solution/insulator interface. Using site-binding theory, a rather simple expression for ψ_0, including the effect of different membrane types, was derived, and according to this model ψ_0 can be expressed as:

$$\Psi = 2.3\frac{kT}{q}\frac{\beta}{\beta+1}\left(\mathrm{pH}_{pzc} - \mathrm{pH}\right) \tag{3.4}$$

where, k is the Boltzmann's constant, T is the absolute temperature, q is the electronic charge, pH_{pzc} is the pH value at which the membrane surface is electrically neutral. Here, β is a factor determining the final sensitivity of the membrane and, as explained in the previous chapter, is the buffer capacity of the insulator surface.

Taking the derivative of equation (3.4) results in the pH sensitivity relation of the ISFET, which is given by equation (2.2). However, it can be seen that the sensitivity parameter α is now replaced with $\beta/(\beta+1)$. This is due to the fact that, for a dilute electrolyte, the effect of the equivalent capacitor C_e can be ignored and the resulting sensitivity depends solely on the type of insulator through β. Examining equation (3.4), reveals that, if the membrane is perfect, the sensitivity parameter β goes to infinity, resulting the term, $\beta/(\beta+1) = 1$. If, now, one calculates the sensitivity of the threshold voltage to pH through ψ_0 as:

$$\left|\frac{\partial \psi_0}{\partial \mathrm{pH}}\right| = 2.3\frac{kT}{q}\Big|_{T=20^{\circ}C} \cong 58.2 \text{ mV/pH} \tag{3.5}$$

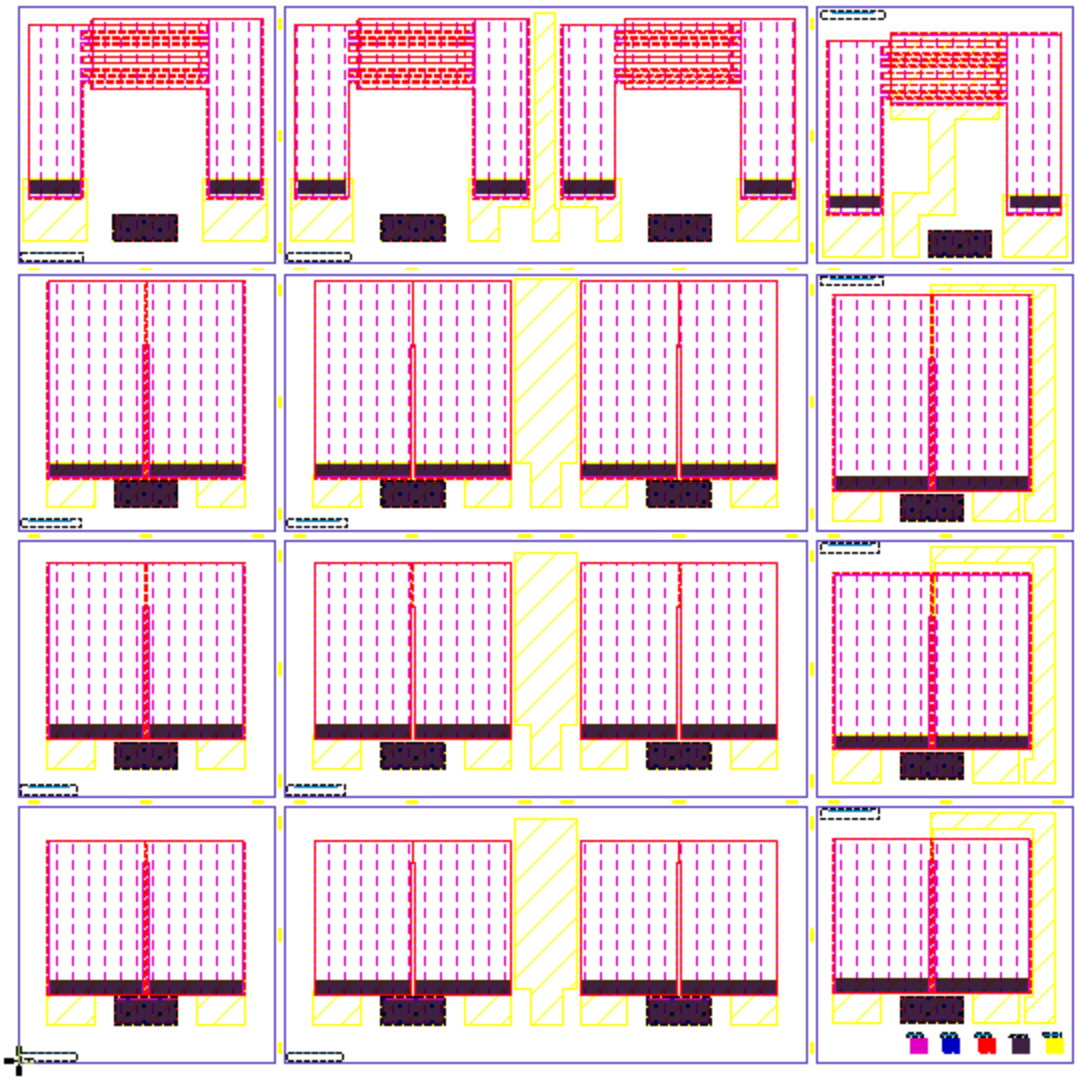

Figure 3.3: Mask design for ISFET test structures.

3.2. ISFET Fabrication

Most ISFETs are processed using standard CMOS technologies; therefore, they are planar devices with source and drain connections at the same side as the gate. The only difference occurs, when it comes to selecting the gate dielectric since the actual sensitivity is determined by this layer. This layer is deposited usually on top of the

already existing gate oxide. In this study, as mentioned earlier, the choice of membrane is Si_3N_4 which is readily available in CMOS process here at RIT.

Figure 3.3 illustrates the mask designed for fabricating the test structures. The chip size is 20x20 mm and includes 4 different sizes of ISFET structures having (*W*/*L*) [µm/µm] ratios of 400/20, 800/40, 1200/60 and 20,000/20 (interdigitated). In addition to these single ISFETs, a pair of each device was repeated in the mid-column of the layout together with integrated Au reference electrodes in between to accomplish fully integrated sensors. The last column of the mask includes MOSFET devices that are structurally same as ISFETs except there are metal gate electrodes on top. The ISFET process was realized using RIT's MEMS process. It is composed of 5 lithography levels. The process-flow steps are provided in Table 3.1. The gate dielectric formed by a 150 Å of SiO_2 with a 1000 Å of Si_3N_4 membrane. The final cross-section of the simulated device is illustrated in Figure 3.4.

Table 3.1: ISFET Process Flow

#	Process Step	Recipes & Conditions
1	P-type Wafers	6" (150 mm) wafers, p-type, 19.5 Ohm-cm
2	RCA clean	Normal
3	Grow 500A pad oxide	Tube 4, recipe 250, 1000C
4	1500A LPCVD nitride	Recipe FAC810
5	Photo 1: Active	Coatmtl.rcp, Devmtl.rcp, 200 mJ/cm2
6	Etch 1500A nitride	Lam 490. End point. FACNIT
7	Channel stop implant	B11, 8E13 cm-2, 100 keV
8	Strip resist	Branson asher, 6" Factory
9	RCA clean	Normal
10	Grow 6500A LOCOS	Tube 1, recipe 406, 1100C
11	Wet etch 1500A nitride	60 sec HF dip, 45 min hot phos
12	Etch 500A oxide	10:1 BOE, 1 minute
13	Grow 1000A Kooi oxide	Tube 1, recipe 311, 900C
14	**Optional channel implant	No mask, P31, 0 to 1E12 cm-2, 50 keV
15	Photo 2: P+	P+ contact. coat.rcp, develop.rcp, 180 mJ/cm2
16	P+ Implant	B11, 2E15 cm-2, 50 keV.
17	Strip resist	Branson asher, 6" Factory
18	Photo 3: N+	Drain/source. Coat.rcp, develop.rcp, 180 mJ/cm2

19	N+ Implant	P31, 2E15 cm-2, 60 keV.
20	Strip resist	Branson Asher, 6" Factory
21	RCA clean	Normal
22	Implant anneal	Recipe 105, Tube 2, N2, 1000C
23	Etch 1000A oxide	10:1 BOE, 2 minutes
24	Grow 150A gate oxide	Tube 4, recipe 215, 900C
25	LPCVD nitride	1000A gate nitride. FAC810
26	Photo 4: CC	coat.rcp, develop.rcp, Dose=____?
27	Etch 1000A nitride	Lam 490. End point. FACNIT
28	Etch 150A CC oxide	BOE 10:1 w/surfactants, 30 seconds
29	Strip resist	Branson Asher, 6" Factory
30	Special RCA clean	RCA clean with extra HF dip at the end.
31	Metal 1 - Gold	Evaporate 2000A gold
32	Photo 5: Metal	coat.rcp, develop.rcp, Dose=180 mJ/cm2
33	Etch 2000A gold	Wet etch, chemicals? Etch rate?
34	Strip resist	Branson Asher, 6" Factory
35	Test	
36	Sinter (optional)	Recipe 101, 450C, H2N2, 30 min

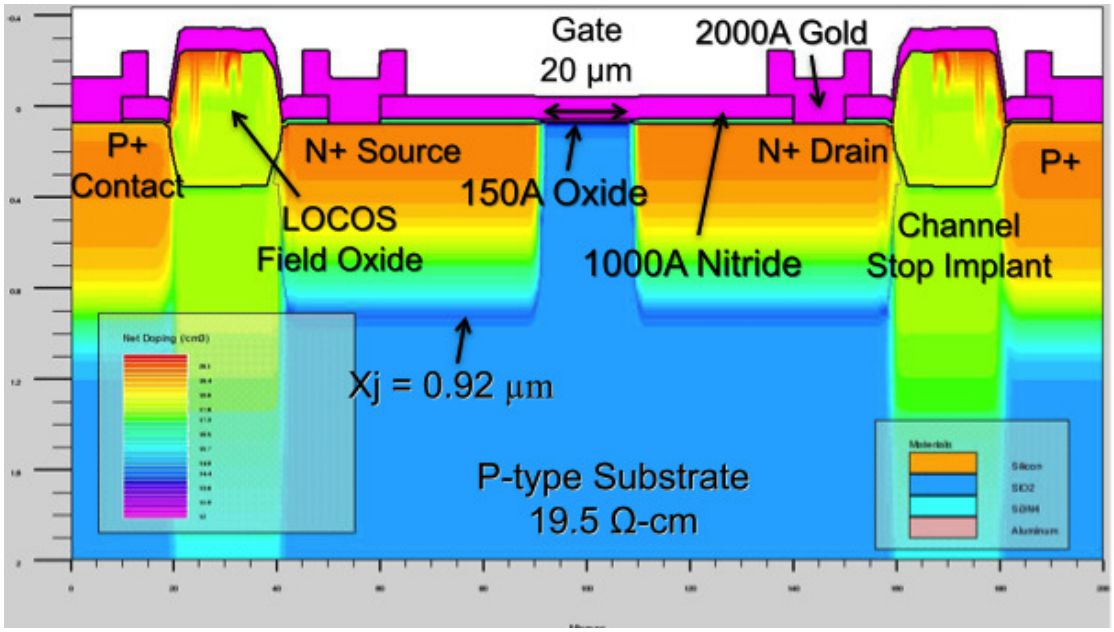

Figure 3.4: Final cross-section of the simulated ISFET device.

The process simulation was performed in Silvaco's Athena tool. The devices were processed on four 6″ wafers, with an average resistivity of 19.5 Ω_cm, and each wafer received a different threshold adjustment implant. The transistors were laid out such that the drain/source contacts were extended away from the gate area as much as possible (2.5 mm), since the metal contacts had to be isolated from the sensing gate which would be in contact with the test solution. However, to decrease the series resistance of source and drain resistance these extended regions were implemented as wide as possible (1.8 mm) resulting in a lower sheet resistance. These dimensions are shown on a single ISFET device in Figure 3.5. In addition, to prevent any oxide breakdown upon contact

with the electrolyte, the devices were realized as depletion mode (normally-on) transistors [3].

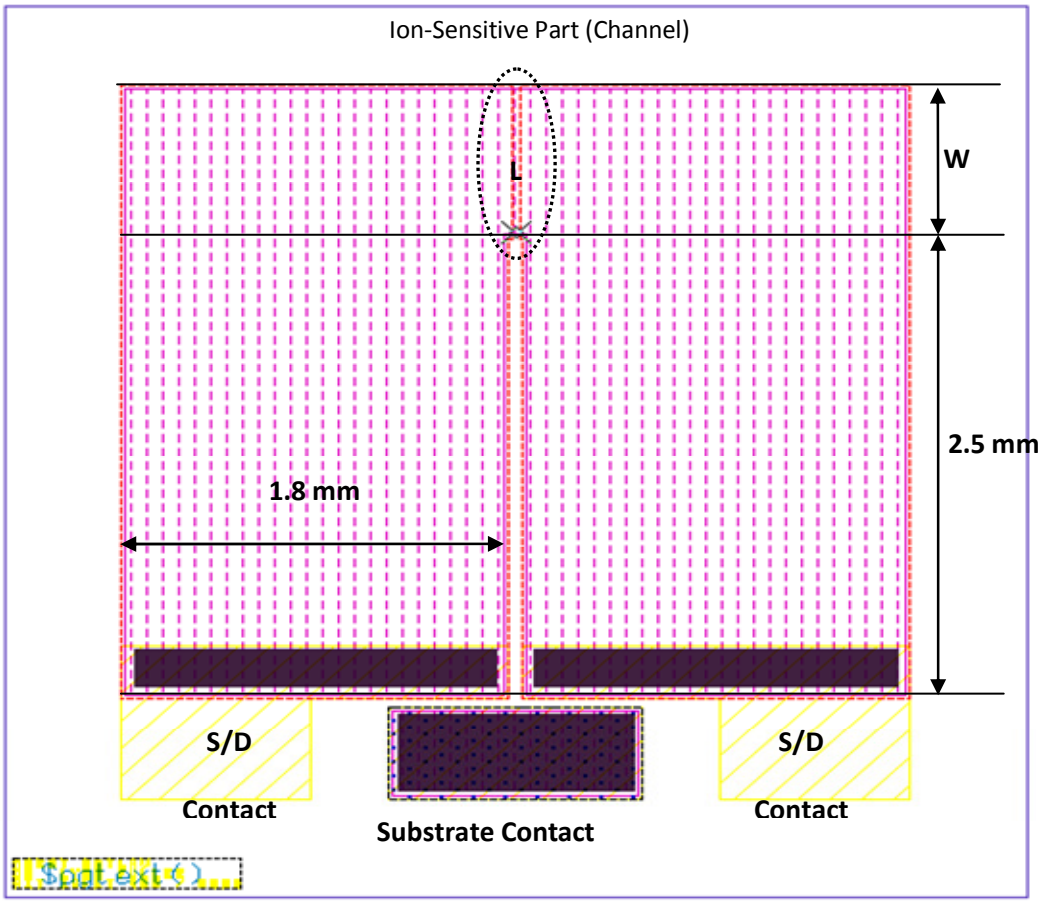

Figure 3.5: Single ISFET with dimensions illustrated for drain and source extensions.

Figure 3.5 illustrate the layout of this source and drain extensions. These extensions are structurally identical for all ISFETs on the mask but the only thing that is changing is their corresponding channel widths. One other benefit of these extensions is that it allows a free working room during the epoxy isolation process, since on the trial

stage of these devices, the gate are is not isolated via using lithography. However, in future designs, it is recommended that an extra mask layer, that will cover the gate area and expose the rest of the structure for isolation process is added to the process flow.

Chapter 4

ISFET Testing and Procedure

4.1. Test Structure Preparation and Test Setup

After the wafers are fully processed, individual ISFET test structures were selected to perform sample preparation prior to electrical testing. As shown in Figure 4.1, fully processed wafers were sawed. In order to determine the specific structures to use, the integrated MOSFET structures went through electrical characterization tests, and Id_Vd and Id_Vg charts were plotted. The tests were done on several MOSFETs across the wafer and it was seen that the threshold voltage of these devices were changing significantly. Later, it was concluded that this was most probably due to the fact that, the wafers had to be kept for a long time outside right after the gate oxide growth process. The CVD tool was not able to deposit the nitride layer right after the gate oxide step, and the wafer surfaces were probably contaminated and thus, introducing shifts in threshold voltages of the FETs across the wafers. This could have been prevented, had the wafers received a modified RCA clean by skipping the HF-dip step.

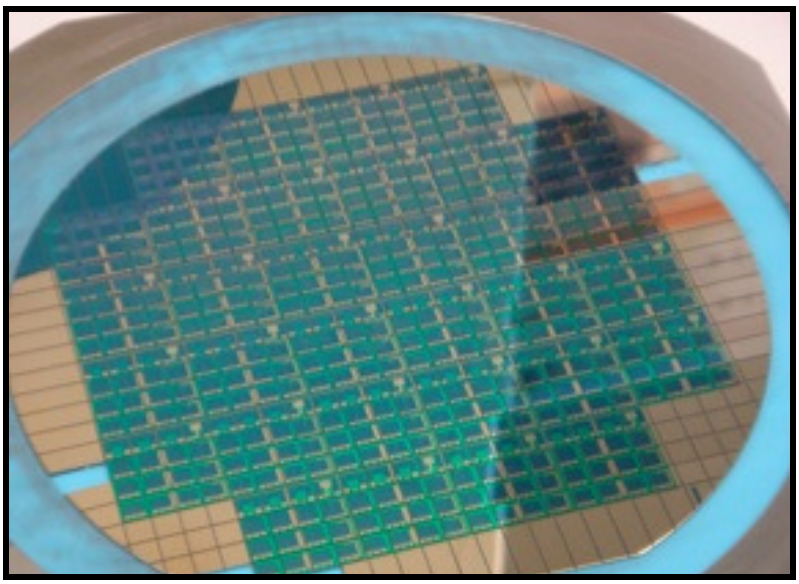

Figure 4.1: Processed wafers were sawed prior to sample pick up.

ISFETs were picked from dice in which the integrated MOSFETs had the lowest threshold voltages. Doing so, helped the biasing of the ISFETs with lower voltages and not exceed ICS station capabilities. Afterwards, the samples were glued via epoxy on dedicated PCB boards, which were conveniently designed thin and long to aid in testing the structures in solutions. Figure 4.2 shows one of the test wafers on a PCB board after this procedure. The epoxy also served as an insulating layer to prevent the solution reaching the source and drain metal contacts of the ISFETs [17]. Because, if these contacts were not isolated, then, in time they will be corroded and more importantly, ISFETs would not be biased only by the reference electrode but also by the drain/source biases.

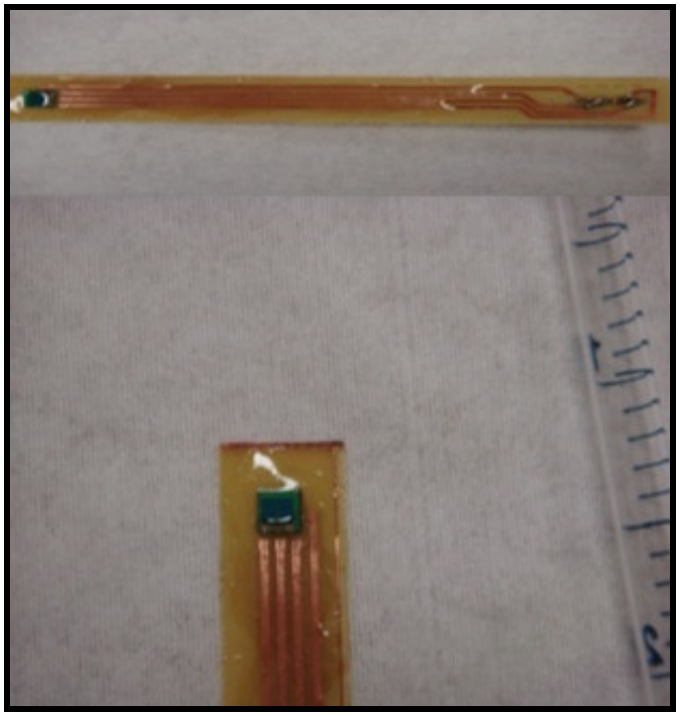

Figure 4.2: ISFET device glued on a dedicated PCB.

In order, to be able to see the shift in the threshold voltages of ISFETs, the EIS system must have a constant and stable gate bias which is provided by the reference electrode, which is also the remote gate electrode of the ISFET. Only then, a change in the potential drop across the insulator surface-electrolyte interface can be compensated by the surface potential of the semiconductor. This is the mechanism that will result in a shift in threshold voltage of the device with respect to the changes in the pH of the bulk solution.

In addition to isolating the source-drain contacts, the corners of the ISFET chip has to be insulated with epoxy as well. Ideally, the only part of the ISFET chip which is exposed to the test solution must be the sensing gate area.

Figure 4.3: Buffer Solutions for pH testing.

Figure 4.3 is showing the buffer solutions which were used in pH sensitivity testing of the ISFET devices. These solution are dilute solutions and convenient to perform the initial tests on the ISFETs. Also, since they are buffer solutions, they are actually resistant to pH changes caused by temperature variations. This property of the buffer solutions came in handy during the temperature testing of the devices. Initially, there were three different buffer solutions, with pH values 4, 7 and 10. However, by mixing these solutions, it was possible to obtain solutions varying between pH 4 to 10. Employing a pH meter also helped monitoring the pH of the solutions during testing in real time. These solutions were also used in calibrating the commercial pH meter in a 2 weeks period. To obtain accuracy in measurements, a 3-point calibration was performed instead of the usual 2-point calibration.

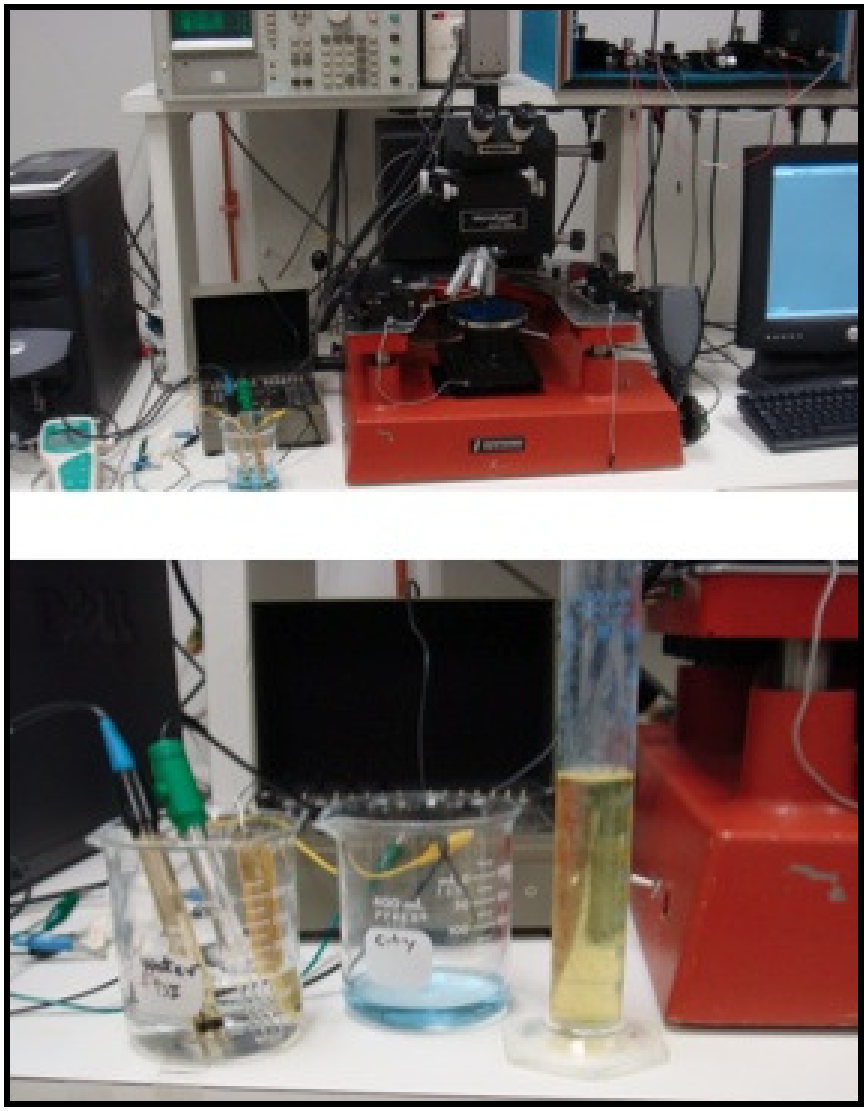

Figure 4.4: ISFET test setup.

Figure 4.4 is an illustration of the test setup used in testing of the ISFETs. The test setup is comprised of HP4145 semiconductor parameter analyzer for biasing and curve extraction through ICS station software interface between the computer and the analyzer. In addition, a Ag/AgCl commercial reference electrode and a Au wire were used to bias

the ISFETs and compare whether, Au could be used as a biasing electrode and therefore, integrated on the chip together with the ISFETs. Test setup also included the pH meter, buffer solutions, beakers, lab-grade NaCl and $NaNO_3$ salts for Cl^- - sensitive membrane testing, DI water and magnetic stirrer to obtain homogeneity throughout the solution.

4.2. pH Sensitivity Tests

Prior to testing, epoxy-isolated ISFET test structures were taken to RIT SMFL facility, where they received a pre-treatment. The sensitive, nitride gate area of the ISFET was exposed to a 50:1 buffered HF solution for about 20 seconds to obtain a pure nitride surface. This is a one-time only treatment. As long as the ISFET structures were kept in DIW for 10 minutes and dried off, the sensitivity will not degrade in time. This was observed as a conclusion since the same ISFET structures were used throughout the project over and over again to obtain repeatability.

Figures 4.5 to 4.8 illustrate the Id_Vg sweeps obtained from the integrated and single ISFET structures. Prior to testing, ISFETs were dipped in the solutions for about 30 minutes to make sure a stable insulator-electrolyte interface was established. After that point, the devices can be removed and dipped in the solutions over and over again. Each curve on the graphs were obtained by waiting about 3 minutes between pH changes.

However, time-based testing results showed that the ISFETs are responding to pH changes faster than this time.

Figure 4.5 is illustrating the Id_Vg sweeps performed on an interdigitated ISFET structure. Drain of the ISFET was kept at V_D= 0.1 V and gate bias, V_G, was swept while measuring the current. The voltage sweeps were performed at 5 different pH values and as can be seen, the resulting curves show that the ISFET is working same as a regular MOSFET device. In addition, the effects of the fringing fields are also obvious in this case, since this device has an interdigitated structure. As the pH value of the solution decreases, the hydrogen ion concentration in the vicinity of the insulator surface decreases. Then, the insulator surface buffer more hydrogen ion in the electrolyte resulting with a net surface charges which is negative. The negative surface charge is screened by more positive charge on the other side of the double layer and this mechanism result in an increased potential drop ψ_0 across the interface.

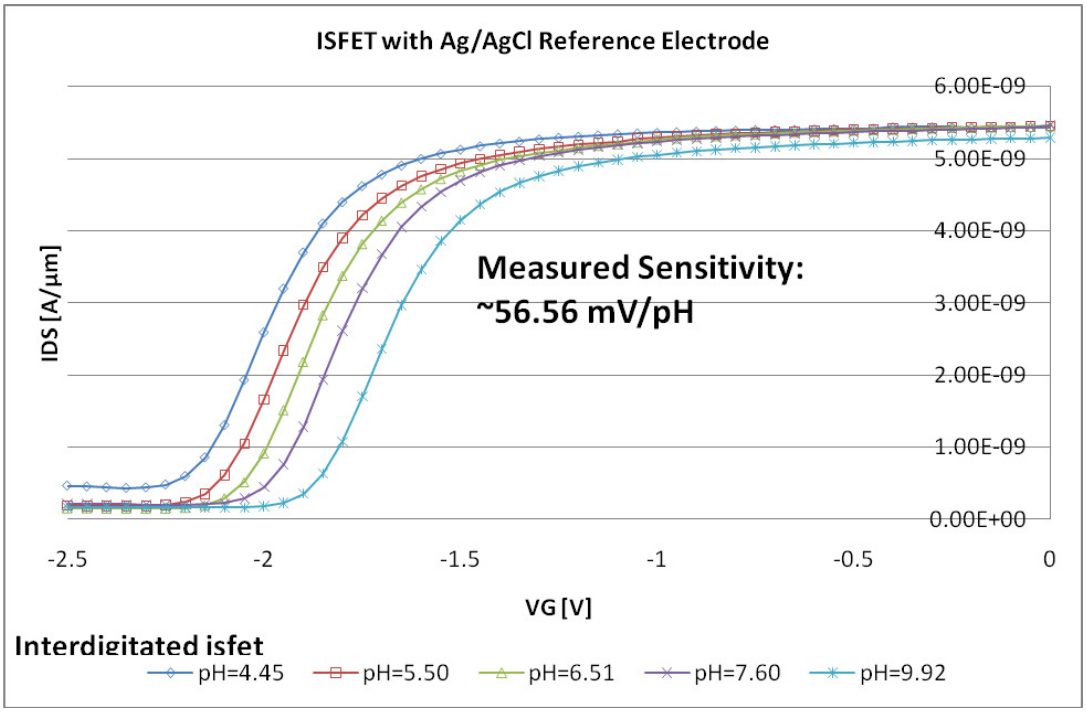

Figure 4.5: Id_Vg sweeps on an interdigitated ISFET biased with a commercial Ag/AgCl electrode.

Since V_D is constant, for a constant value of V_G, the increase in the ψ_0 has to be compensated by a decrease in the surface potential, ψ_s, of the semiconductor. This mechanism results in a decrease on the threshold voltage as can be seen from the graph. The sensitivity of the ISFET threshold voltage to the changes in pH of the solution was calculated simply by extracting the threshold voltage at each curve for each pH and then by dividing the difference in threshold voltages to the difference in pH values. This resulted in a pH sensitivity of ~ 56.56 mV, which is very close to the Nerst sensitivity.

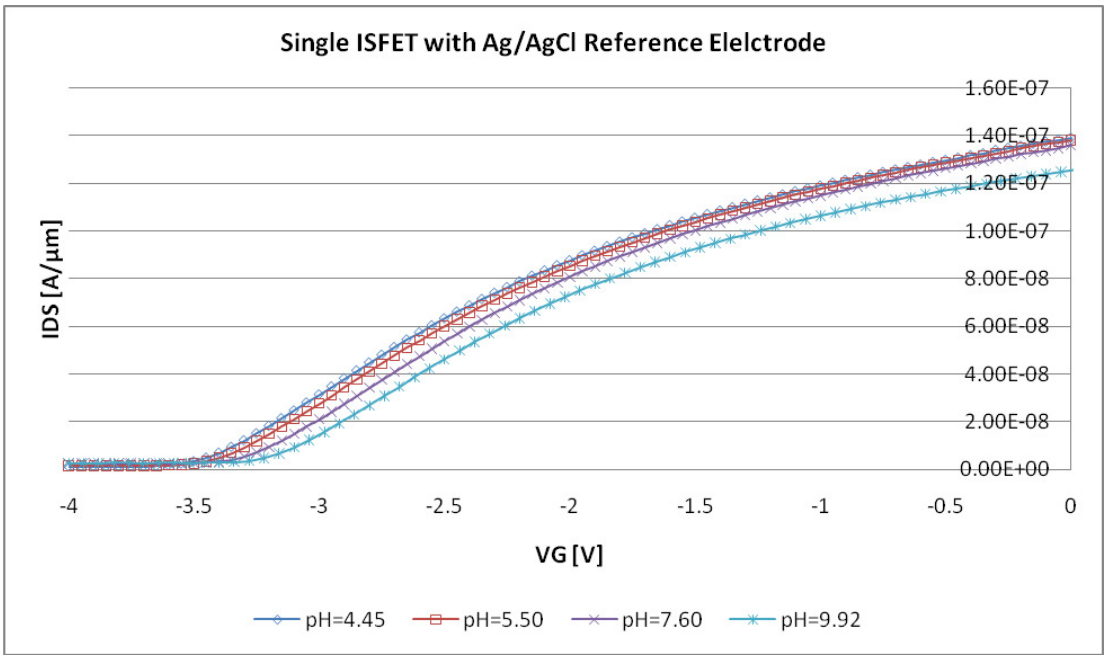

Figure 4.6: Id_Vg sweeps on a single ISFET biased with a commercial Ag/AgCl electrode.

Figure 4.6 is the same experiment, repeated with a single ISFET biased by the commercial electrode. As can be seen, there are 4 curves extracted for the device at 4 different pH values. Device is working just as a MOSFET device but the threshold voltage is shifting with respect to the changes in the pH of the solution. As mentioned earlier, as the pH value of the solution decrease, the threshold voltage of the ISFET is decreasing, as well. In addition, the sensitivity of the device threshold voltage is about the

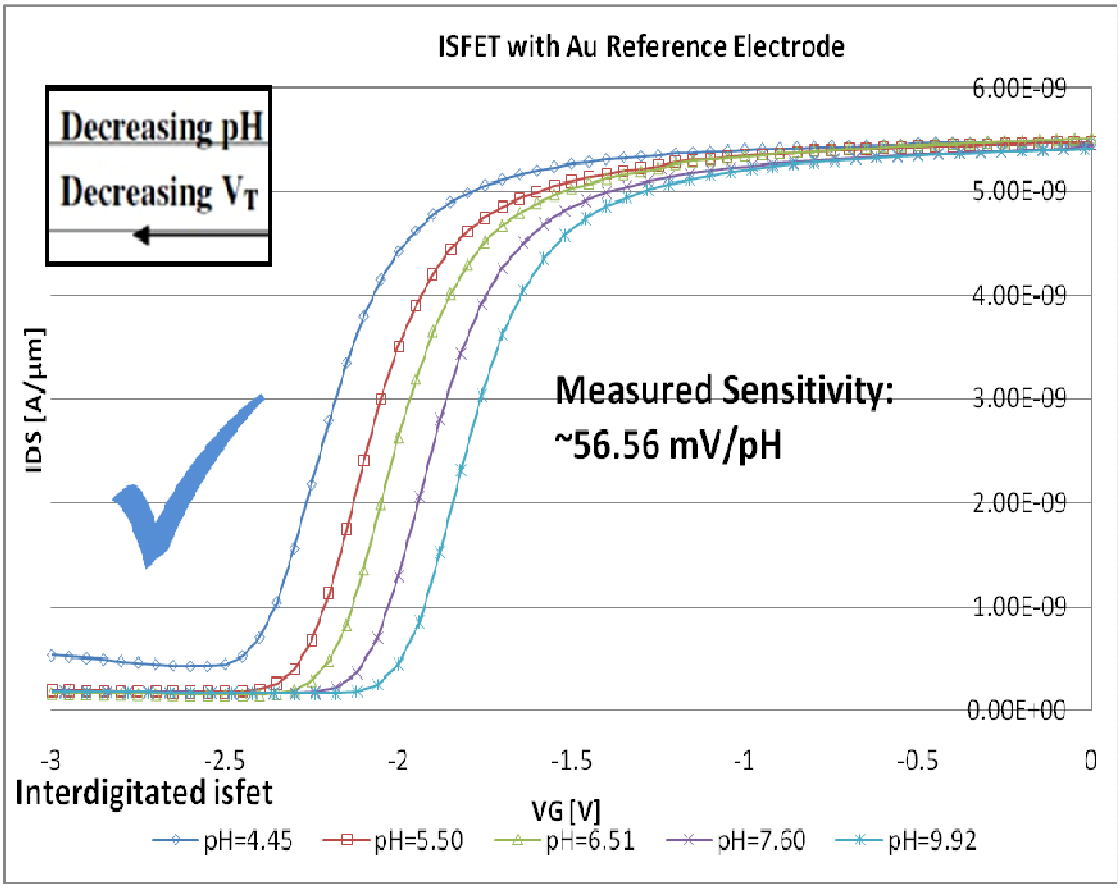

Figure 4.7: Id_Vg sweeps on an interdigitated ISFET biased with an integrated Au electrode.

same as the interdigitated device of Figure 4.5. Even though, these devices are coming from the same wafer, their threshold voltages are different. This is due to the fact that the devices were picked from different dice on the wafer, and as mentioned previously, there is a threshold variation across the wafers.

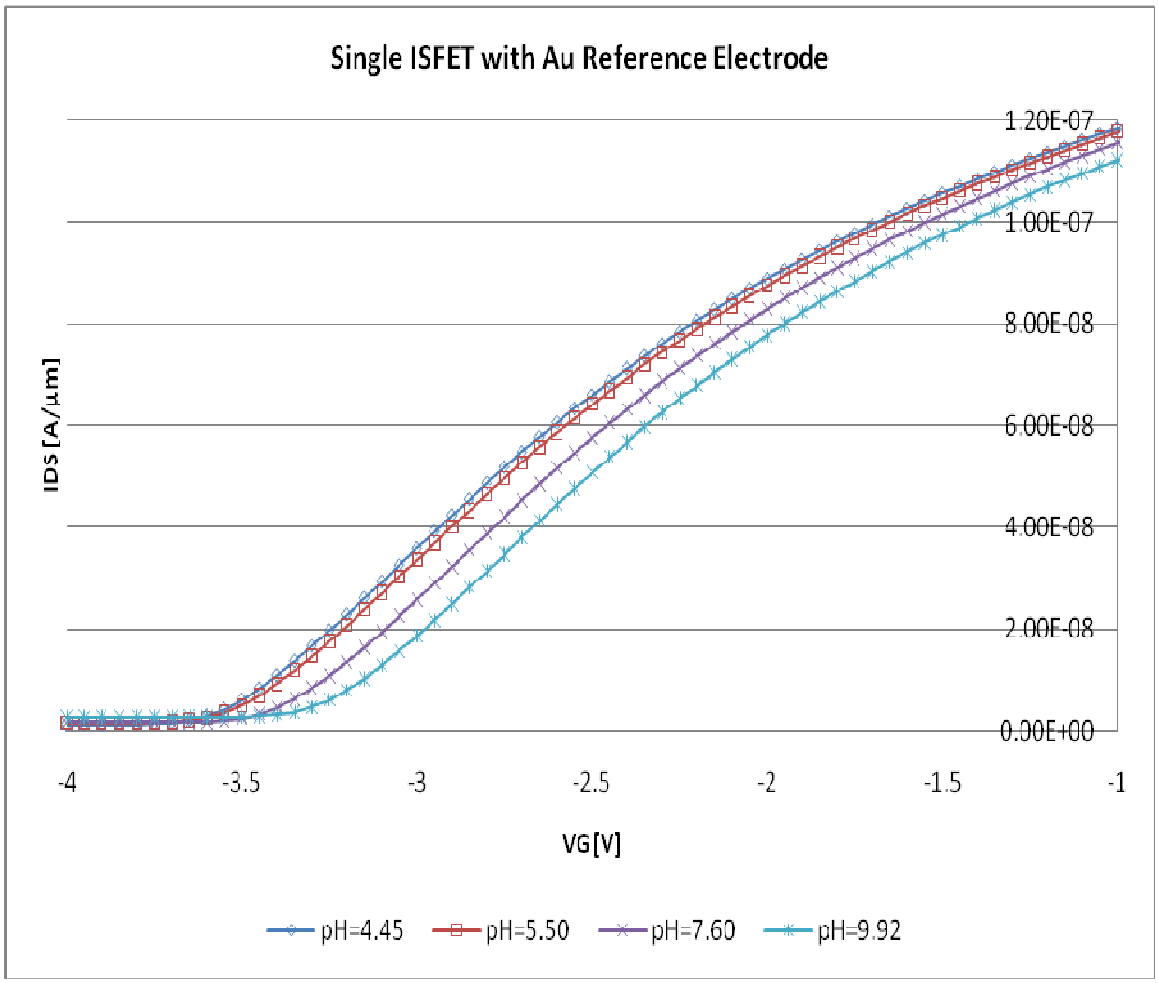

Figure 4.8: Id_Vg sweeps on a single ISFET biased with an integrated Au reference electrode.

Figure 4.7 is showing the curves extracted from an ISFET with an integrated Au reference electrode. The results from this test are important in a couple of aspects. First, Au metal is able to bias the ISFET same as the commercial reference electrode with a slight shift in the threshold voltages due to the work function difference. Second, the fact that the experiment is done with an integrated Au electrode on the wafer, shows that ISFETs can be fully integrated with signal conditioning circuits since there is no need of a bulky reference electrode. In a multisensory system, the ISFET provides full and

compact integration. Third, the threshold voltage sensitivity to pH is the same as in the case of Figure 4.5 since the work function is a constant parameter and therefore cancels out during sensitivity calculation.

Finally, Figure 4.8 is illustrating the results obtained from the same single ISFET used in the case of Figure 4.6. Same comments would apply for these results too if the two cases were compared. Other than the slight shift in the threshold voltages, the curves are the same as well as the sensitivity of the threshold voltages to the changes in the pH of the bulk solution.

4.3. Chloride Ion Sensitivity Tests

As explained in Chapter 3, pH sensitive ISFETs can be made sensitive to other ions of interest with a dedicated membrane covering the pH sensitive insulator of the device. Therefore, the ISFET is made sensitive to the ion of interest which causes a local pH change in the membrane by reacting with the hydrogen ions.

In order to achieve a Cl^- -sensitive ISFET, a dedicated membrane was prepared and applied over the nitride gate area of the ISFETs. The membrane recipe of [14] was employed for this purpose only with a possible slight difference in the amount of reagents. The reagents used to prepare this membrane are given in Table 4.1.

Table 4.1: Cl^- -sensitive membrane reagents and amounts.

Reagent	Function	Amount
RT 3140-Silicon Rubber	Forms the membrane matrix	0.3 gr
MnTPPCl-Ionophore	Responsible for Cl^- transfer into the membrane	0.01 gr
TDMACL-Ionophore	Responsible for Cl^- transfer into the membrane	0.01 gr
NPOE-Plasticizer	Adhesion and durability promoter	0.1 gr
Tetrahydrofuran-Solvent	Required to dissolve the reagents	0.4 ml

As can be seen in Figure 4.9, the membrane was prepared in clean room environment here at RIT. All the membrane reagents were mixed and dissolved in tetrahydrofuran and mixed with a stirrer. Afterwards, the prepared membrane solution was injected on top of the nitride gate area of the ISFETs and the devices were left in the clean room for 24 hours of solvent dry off. The ISFETs used for this experiment are different devices than the ones used in pH testing. Therefore, prior to applying the membrane the devices went through the same 50:1 buffered HF dip step.

After the solvent dry off, devices were taken to the test lab for Cl^- sensitivity testing. For these tests, lab-grade NaCl and $NaNO_3$ salts were dissolved in DI water to prepare 0.1M and 1M solutions of Cl^- solutions. Tests also were performed in a solution of 0.1M NaCl in which the same amount of NO_3^- was added by dissolving $NaNO_3$. This is done to make sure that the membrane is only and/or mostly sensitive to the Cl^- ions. Prior to testing, devices were kept in the solutions for about 45 minutes. The longer time

compared to the pH testing case is due to the fact that only after this amount of time, Id_Vg and Id_Vd curves could be extracted. The extractions were performed in the "long integration mode" of the HP4145 semiconductor parameter analyzer.

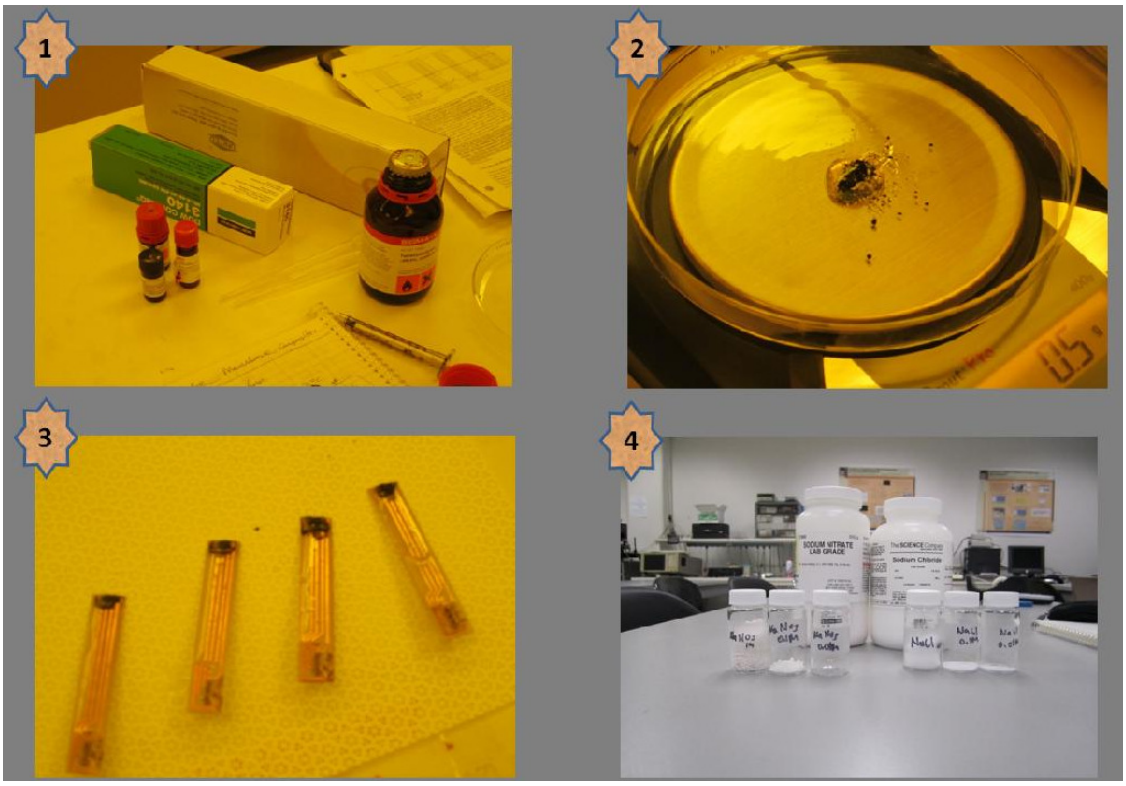

Figure 4.9: Cl^- -sensitive membrane preparation steps.

Figures 4.10 to 4.12 illustrate the Cl^- sensitivity testing of a single ISFET with integrated Au reference electrode. As can be seen from Figure 4.10, the threshold voltage of the ISFET was shifted as the Cl^- concentration was varied from 0.1M to 1M. As the Cl^- concentration is increased, the amount of Cl^- in the vicinity of the nitride surface. These

ions react with hydrogen ions and reduce their concentration, resulting in a basic solution here. Just like in the case of a pH sensitive ISFET, the threshold voltage of the device increases as the solution gets more basic or in other words, has a higher pH.

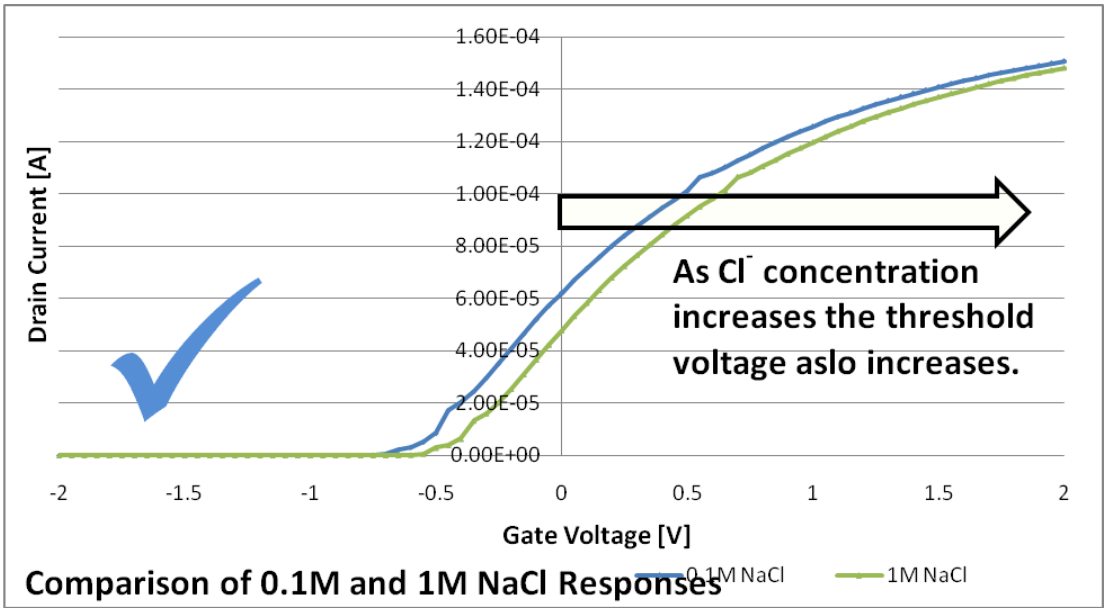

Figure 4.10: Threshold voltage shift of ISFETs with respect to Cl^- concentration change.

Figure 4.11 illustrates the output characteristics of the Cl- -sensitive ISFET response. Output characteristics were plotted for both 0.1M and 1M Cl^- solutions on the same plot. Here, the effect of threshold voltage shift can be observed extremely well by looking at the saturation currents. Saturation drain currents for the ISFET are higher for the 0.1M NaCl due to the lower threshold voltage which was observed in Figure 4.10. Threshold voltage sensitivity of the ISFET device was found to be ~100 mV/pCl.

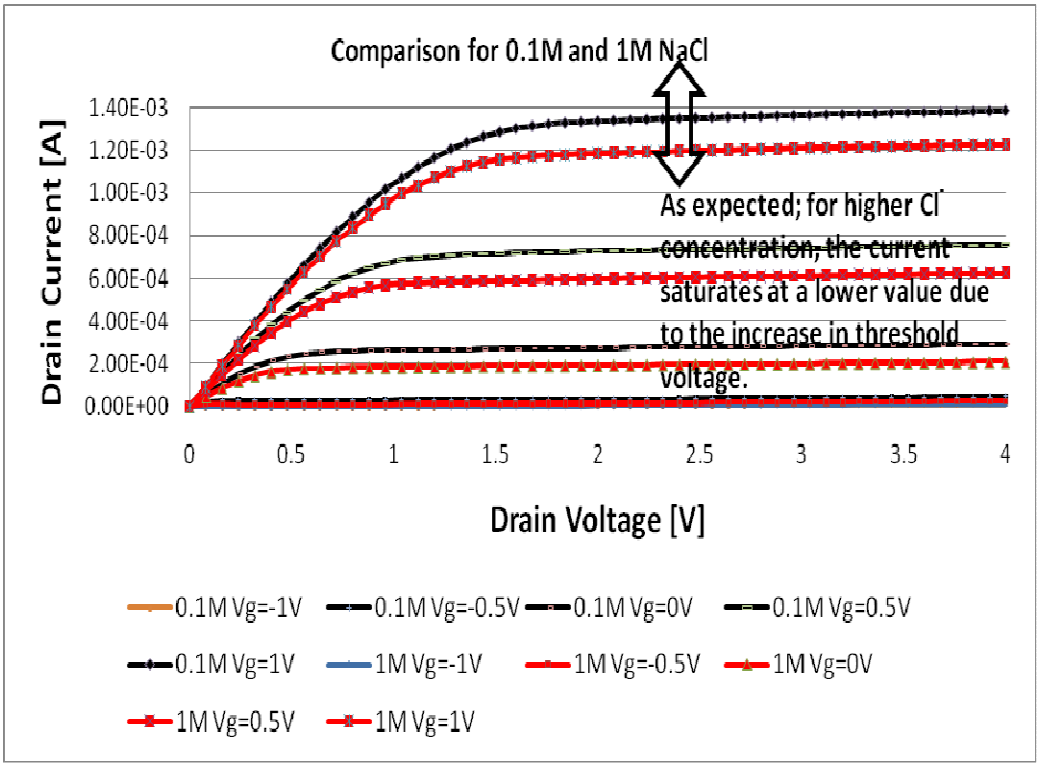

Figure 4.11: Output characteristics of the ISFET in 0.1M and 1M NaCl solutions.

Figure 4.12 is showing the results for the case where 0.1M of NO_3^- ions was added to a solution in which 0.1M of Cl^- ions resided. In this case, the change in the amount of saturation drain current is very little. One important observation is that, even though the amount of negative ions doubled, the saturation current is following an increasing behavior. If the membrane was actually allowing NO_3^- ions to come close to the nitride surface, then one would expect the threshold voltage to increase even more, then, for which a lower current would be observed. One guess that needs to be proven is that, adding $NaNO_3^-$ salt to the solution is actually increasing the Na^+ content, as well. It is possible that the excess Na^+ is decreasing the Cl^- content, therefore resulting in a lower

threshold voltage, which would explain the higher current. If this is really what is happening, then, the membrane is rejecting the NO_3^- and the shift in the threshold voltage is only due to the change in the Cl^- concentration. However, this theory needs to be proved through further experiments and research.

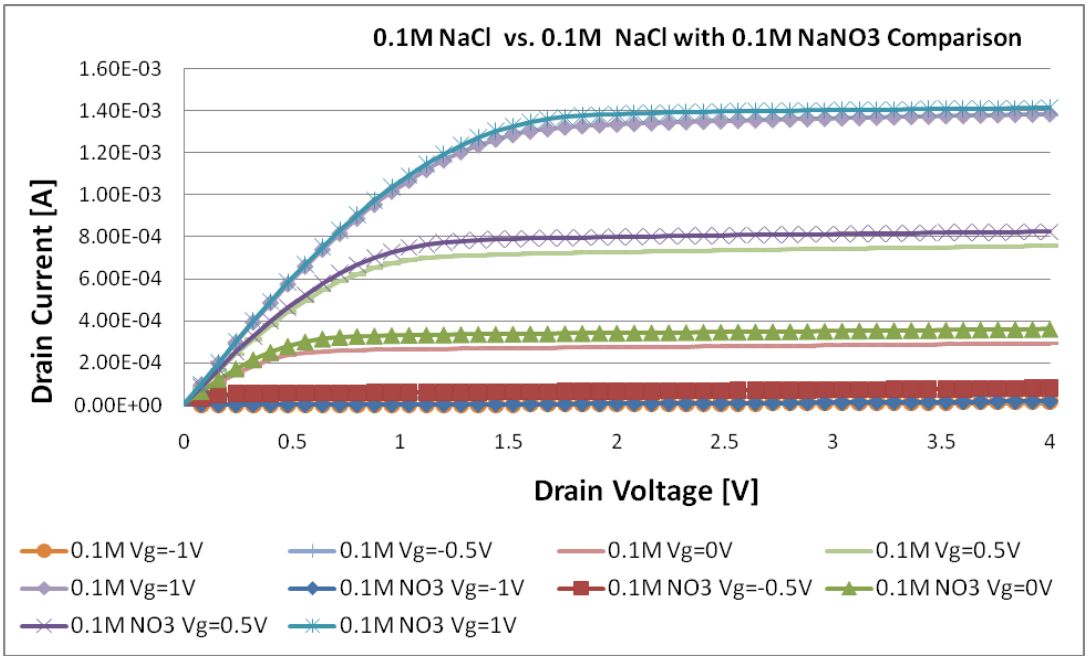

Figure 4.12: Testing the membrane sensitivity to NO_3^+.

4.4. Long-Term Drift Tests of the ISFET

Long-term drift tests were performed to investigate whether the threshold voltage of the ISFETs would shift with respect to long-term exposure to test solutions. In order to do so, ISFETs were soaked in solutions with different pH values and biased at non-saturation. Devices were biased at the middle of the linear portion of the Id_Vg curves.

Figure 4.13 and 4.14 illustrate the tests results of this experiment. As seen in Figure 4.13, ISFETs were dipped in solutions with pH 7 and 10. Due to poor isolation of one ISFET device, the curve for the case of a pH 4-solution could not be obtained. The metal connections of drain and source contact were exposed to solution thus, were biasing the solution together with the reference electrode. ISFETs were biased with the commercial reference electrode and their currents were monitored for 24 hours. Test results show that

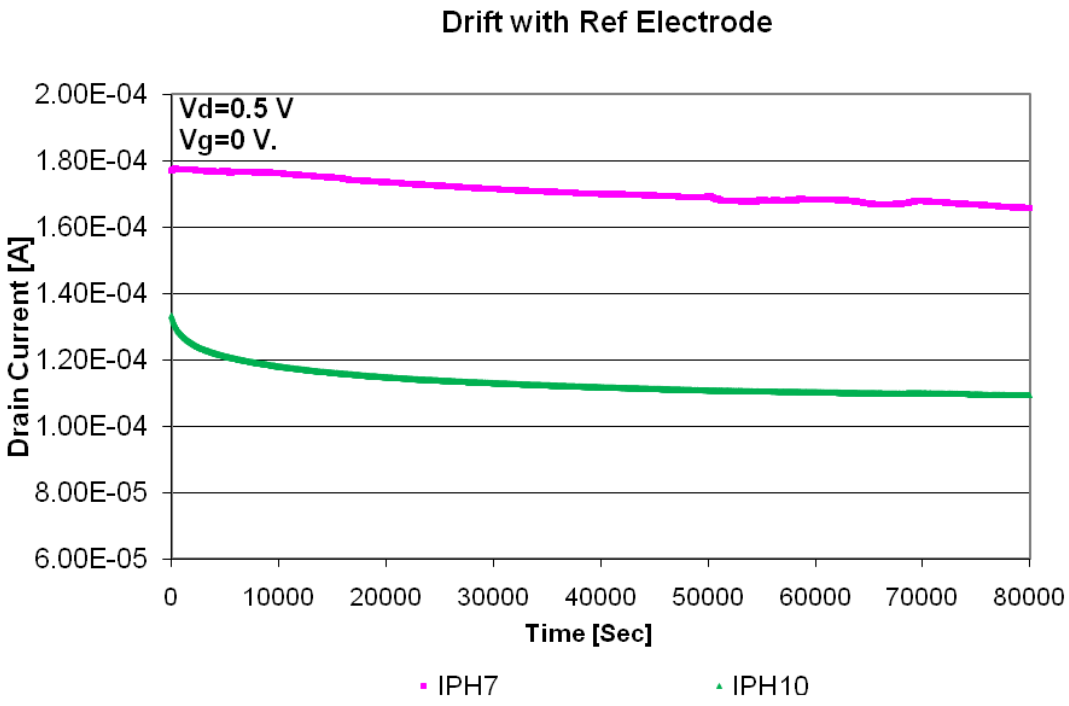

Figure 4.13: Long-term drift of the Ag/AgCl electrode-biased ISFET current in solutions with various pH values.

the change in the current over a day is significantly low. Same conclusions apply to the results in Figure 4.14 where ISFETs were biased by the integrated Au reference electrode. Again, the change in the current is significantly low. This experiment is also

giving an idea about the quality of the nitride layer of the ISFETs. The small drift in the threshold voltage of the ISFETs can be explained by the highly stoichiometric and oxygen free characteristics of the CVD nitride.

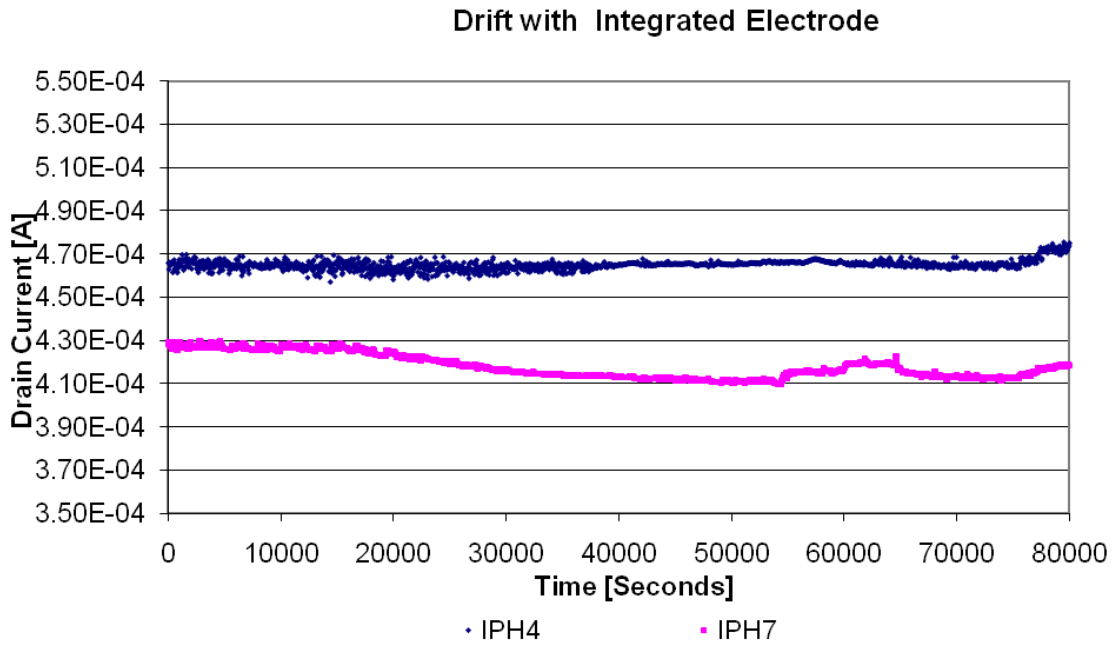

Figure 4.14: Long-term drift of the Au electrode-biased ISFET current in solutions with various pH values.

4.5. Sensitivity vs. Temperature Tests of ISFETs

Examining equation (2.22) reveals that, assuming a first order dependence, the sensitivity of the ISFET threshold voltage to temperature changes come from the sensitivity coefficient which include the thermal voltage term kT/q. Therefore, one would expect the sensitivity of the ISFET to pH to increase with temperature. In order to investigate this, ISFETs were dipped in solutions of different pH and placed in a box

oven. Temperature was increased and the current values of the ISFETs, biased in non-saturation, were observed. During the current measurements, the instantaneous pH values of the solutions were also monitored by the commercial pH meter. In addition, since the test solutions were buffer solutions, their pH values were resistant to temperature changes and did not change significantly. This actually worked in favor of the experiment.

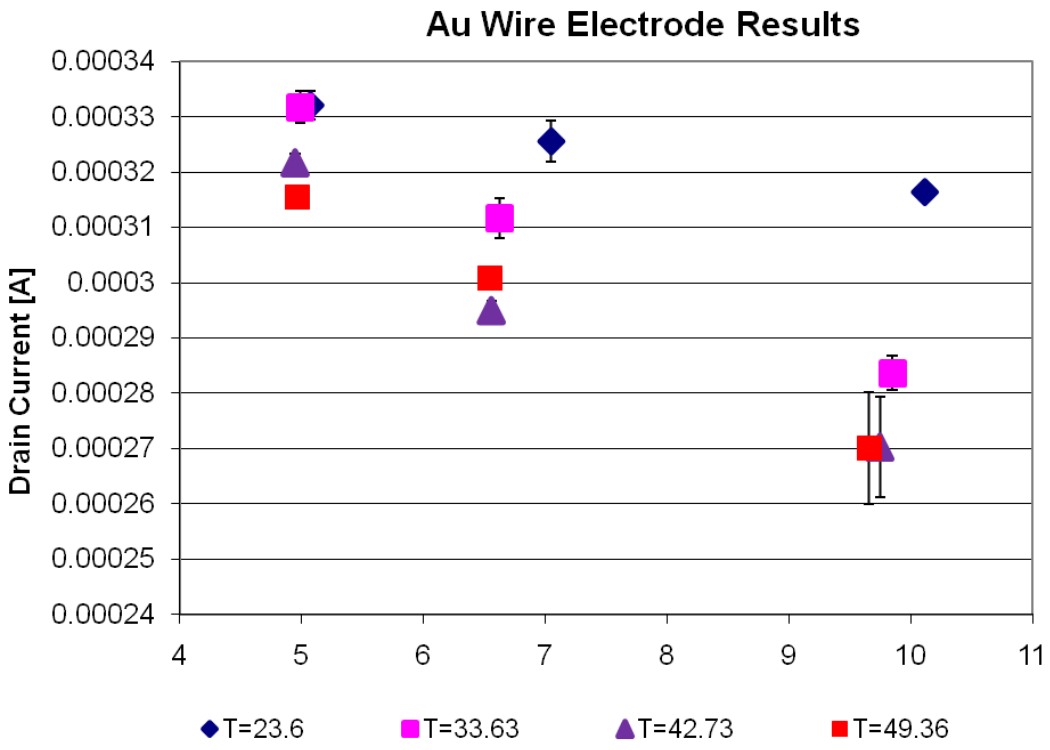

Figure 4.15: Au wire-biased ISFET response to pH change at various temperatures.

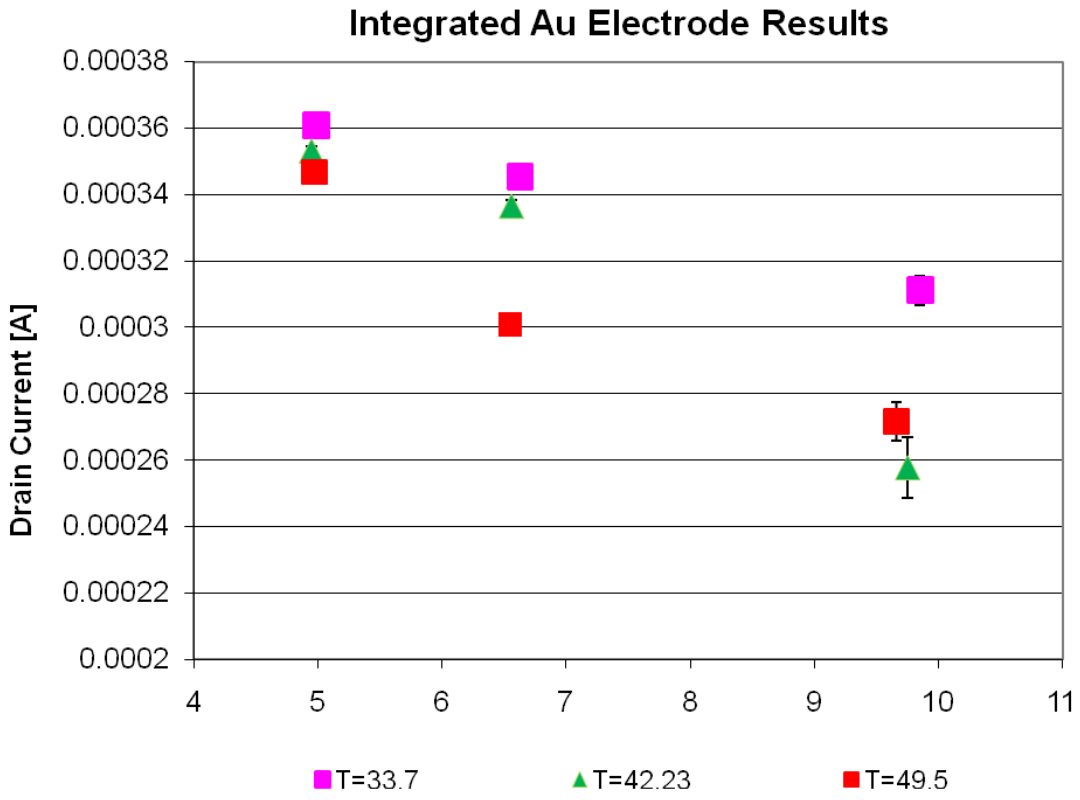

Figure 4.16: Integrated Au electrode-biased ISFET response to pH change at various temperatures.

Figures 4.15 and 4.16 illustrate the results of the temperature tests. For each temperature value, 20 current measurements were taken within 5-minute duration of time. As can be seen, as the temperature increases, the slope of the curve becomes steeper, thus indicating a higher sensitivity of the current to temperature. Also for each temperature and pH value, the variation of the current data stays extremely tight. Here, the figures were plotted only for a Au wire and integrated Au electrode cases. This is due to the fact that, the commercial Ag/AgCl reference electrode was broken during the experiments.

4.6. Time-Based Response of ISFET to pH Changes

Figure 4.17 illustrates the time-based response of the ISFET current, therefore, the threshold voltage with respect to changes on the pH of the solution. For this test ISFET was dipped in a solution and a magnetic stirrer was used to provide a homogenous concentration throughout the solution. The pH of the solution was monitored by the commercial pH meter, as well. As can be seen, ISFET response to pH changes is within seconds if the concentration of the hydrogen ions immediately becomes homogenous throughout the solution after the pH adjustment. In real time applications, where there is not a magnetic stirrer, the response of the ISFET will follow the pace at which the sample solution pH stabilizes. On Figure 4.17, the boxes, which were drawn at transition points, represent the intervals in which the pH of the solution was being adjusted by mixing the solutions with buffer solutions of various pH values. It is seen that, as the pH of the solution increases the value of the current decreases. This result is agreeing perfectly with the theory such that the threshold voltage is increasing with increasing pH. In addition,

when the pH is recovered to the same value as before, the threshold voltage, as well as

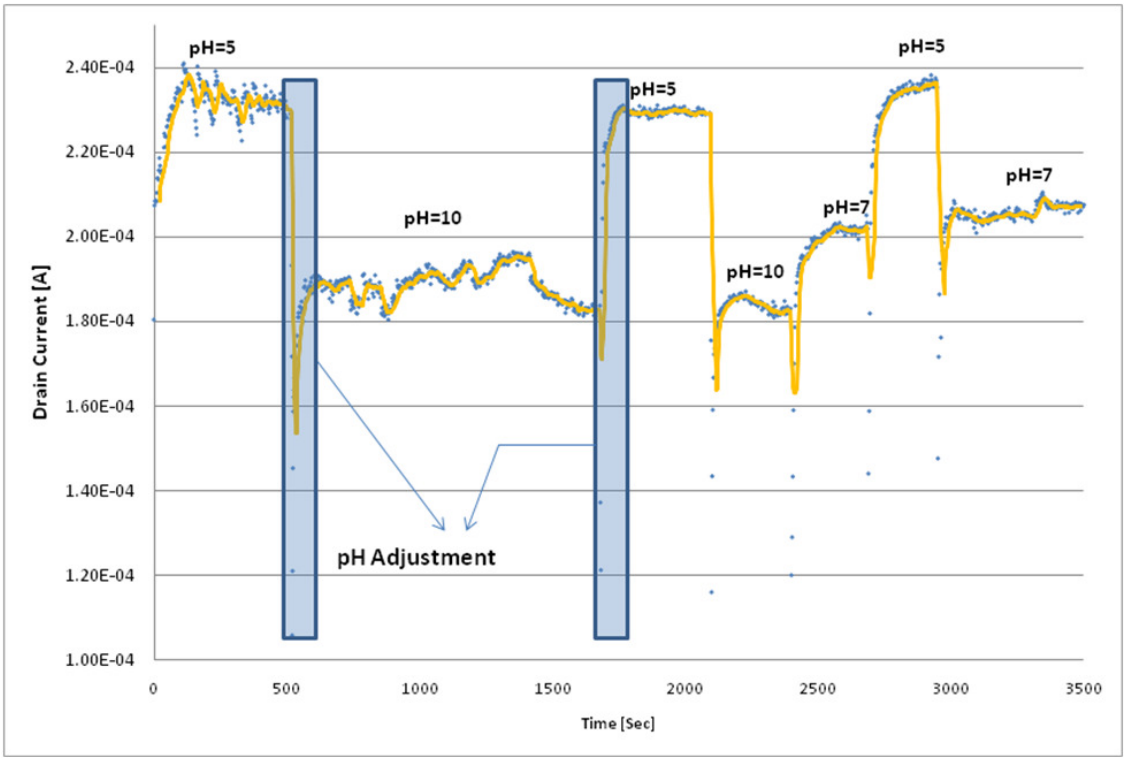

Figure 4.17: ISFET time-based current response to pH changes.

the current, is being recovered to where they were used to be for that same pH. There might be some slight differences due to the fact the pH values that were recovered are not exactly the same values as they were, due to the tedious adjustment procedure. Finally, the graph is indicating fluctuations at current values with time; however, this is due to the magnetic stirrer noise and should be ignored.

Chapter 5

Conclusions on the Study

Test results presented in Chapter 4 show promising and very good results on this thesis study. ISFET devices fabricated here at RIT can be used in both pH and chloride sensing applications. Experimental results agree very well with the literature. For pH sensing applications, the sensitivity of the ISFETs are ~56.56 mV/pH and very close to the Nernstian sensitivity, which is 58.2 mV/pH at 20 °C.

Chloride sensitive membrane, which is prepared at RIT SMFL facility is working extremely well and test results indicate a sensitivity of ~100 mV/pCl. In addition, since the ISFETs are working as pH sensitive devices, the application of these devices is not limited only to chloride ions but other ions can be also investigated with dedicated membranes.

Long-term drift tests are also satisfying, since the drift in the current value over time is significantly low. This is also a proof of the quality of the nitride layer deposited on top of the silicon dioxide layer.

Temperature tests are also agreeing with the theory, such that when the temperature is increased the sensitivity coefficient is also increasing with it. Using the

ISFETs together with a proper signal conditioning circuitry will result in high performance and accuracy applications.

Time-based measurement results show that, as long as the pH value of the solution reaches to equilibrium, ISFETs respond to the pH change within seconds and give a stable signal output. Overall, this study is a success in its field and will open up a path to other thesis topics to follow here at RIT.

References

[1] P. Bergveld, "Development of an Ion-Sensitive Solid-State Device for Neurophysiological Measurements," *Biomedical Engineering, IEEE Transactions on,* vol. BME-17, pp. 70-71, 1970.

[2] P. Bergveld, "Development, Operation, and Application of the Ion-Sensitive Field-Effect Transistor as a Tool for Electrophysiology," *Biomedical Engineering, IEEE Transactions on,* vol. BME-19, pp. 342-351, 1972.

[3] P. Bergveld, "Thirty years of ISFETOLOGY: What happened in the past 30 years and what may happen in the next 30 years," *Sensors and Actuators B: Chemical,* vol. 88, pp. 1-20, 2003.

[4] D. E. Yates, S. Levine, and T. W. Healy, "Site-binding model of the electrical double layer at the oxide/water interface," *Journal of the Chemical Society, Faraday Transactions 1: Physical Chemistry in Condensed Phases,* vol. 70, pp. 1807-1818, 1974.

[5] L. Bousse, N. F. De Rooij, and P. Bergveld, "Operation of chemically sensitive field-effect sensors as a function of the insulator-electrolyte interface," *Electron Devices, IEEE Transactions on,* vol. 30, pp. 1263-1270, 1983.

[6] M. Waleed Shinwari, M. Jamal Deen, and D. Landheer, "Study of the electrolyte-insulator-semiconductor field-effect transistor (EISFET) with applications in biosensor design," *Microelectronics Reliability,* vol. 47, pp. 2025-2057, 2007.

[7] T. Matsuo and K. D. Wise, "An Integrated Field-Effect Electrode for Biopotential Recording," *Biomedical Engineering, IEEE Transactions on,* vol. BME-21, pp. 485-487, 1974.

[8] M. Yuqing, G. Jianguo, and C. Jianrong, "Ion sensitive field effect transducer-based biosensors," *Biotechnology Advances,* vol. 21, pp. 527-534, 2003.

[9] P. Bergveld, R. E. G. van Hal, and J. C. T. Eijkel, "The remarkable similarity between the acid-base properties of ISFETs and proteins and the consequences for the design of ISFET biosensors," *Biosensors and Bioelectronics,* vol. 10, pp. 405-414, 1995.

[10] R. E. G. van Hal, J. C. T. Eijkel, and P. Bergveld, "A general model to describe the electrostatic potential at electrolyte oxide interfaces," *Advances in Colloid and Interface Science,* vol. 69, pp. 31-62, 1996.

[11] P. Delahay, *Double Layer and Electrode Kinetics*. New York: Interscience Publishers, 1965.

[12] E. Gileadi, E. Kirowa-Eisner, and J. Penciner, *Interfacial Electrochemistry: An experimental Approach*. Massachusetts: Addison-Wesley Publishing Company, Inc., 1975.

[13] P. A. Hammond, D. R. S. Cumming, and D. Ali, "A single-chip pH sensor fabricated by a conventional CMOS process," in *Sensors, 2002. Proceedings of IEEE*, 2002, pp. 350-355 vol.1.

[14] A. Bratov, N. Abramova, and C. Domínguez, "Investigation of chloride sensitive ISFETs with different membrane compositions suitable for medical applications," *Analytica Chimica Acta,* vol. 514, pp. 99-106, 2004.

[15] Y.-L. Chin, J.-C. Chou, T.-P. Sun, W.-Y. Chung, and S.-K. Hsiung, "A novel pH sensitive ISFET with on chip temperature sensing using CMOS standard process," *Sensors and Actuators B: Chemical,* vol. 76, pp. 582-593, 2001.

[16] M. Paluch, "Electrical properties of free surface of water and aqueous solutions," *Advances in Colloid and Interface Science,* vol. 84, pp. 27-45, 2000.

[17] W. Oelßner*, et al.*, "Encapsulation of ISFET sensor chips," *Sensors and Actuators B: Chemical,* vol. 105, pp. 104-117, 2005.